NETWORKS AND HETEROGENEOUS MEDIA
©American Institute of Mathematical Sciences
Volume **9**, Number **3**, September **2014**
doi:10.3934/nhm.2014.9.383
pp. **383–416**

COMPUTING THE ASYMPTOTIC SPECTRUM FOR NETWORKS REPRESENTING ENERGY LANDSCAPES USING THE MINIMUM SPANNING TREE

Maria Cameron

University of Maryland
Department of Mathematics
College Park, MD 20742-4015, USA

(Communicated by Benedetto Piccoli)

Abstract. The concept of metastability has caused a lot of interest in recent years. The spectral decomposition of the generator matrix of a stochastic network exposes all of the transition processes in the system. The assumption of the existence of a low lying group of eigenvalues separated by a spectral gap has become a popular theme. We consider stochastic networks representing potential energy landscapes whose states and edges correspond to local minima and transition states respectively, and the pairwise transition rates are given by the Arrhenuis formula. Using the minimal spanning tree, we construct the asymptotics for eigenvalues and eigenvectors of the generator matrix starting from the low lying group. This construction gives rise to an efficient algorithm suitable for large and complex networks. We apply it to Wales's Lennard-Jones-38 network with 71887 states and 119853 edges where the underlying energy landscape has a double-funnel structure. Our results demonstrate that the concept of metastability should be applied with care to this system. For the full network, there is no significant spectral gap separating the eigenvalue corresponding to the exit from the wider and shallower icosahedral funnel at any reasonable temperature range. However, if the observation time is limited, the expected spectral gap appears.

1. **Introduction.** In this work we consider stochastic networks with detailed balance where the pairwise transition rates are of the form

$$L_{ij} = \begin{cases} \frac{k_{ij}}{k_i} e^{-(V_{ij}-V_i)/T}, & \text{if } i \sim j, \\ 0, & \text{otherwise,} \end{cases}, \quad \text{where} \quad i \neq j. \tag{1}$$

Networks of this kind represent, e.g., potential energy landscapes where all critical points are isolated. The set of states is equivalent to the set of local minima, and the set of edges is equivalent to the set of transition states or Morse index one saddles separating the local minima. States i and j are connected by an edge (i, j) (notation $i \sim j$) if and only if the corresponding local minima are separated by a single saddle[1]. The number V_{ij} in Eq. (1) is the potential at the saddle ij separating i and j, V_i is the potential at the minimum i, k_{ij} and k_i are temperature-independent prefactors defined by the Hessian matrices and the orders of the point groups of the saddle

2010 *Mathematics Subject Classification.* Primary: 65C50, 60J27; Secondary: 60J28.

Key words and phrases. Minimum spanning tree, optimal W-graph, asymptotic spectrum, Freidlin's cycle, metastability, Lennard-Jones cluster.

The author is supported by NSF grant 1217118 and DARPA YFA grant N66001-12-1-4220.

ij and the minimum i respectively [29]. T is the temperature, a small parameter. Eq. (1) defines the off-diagonal entries of the generator matrix L while its diagonal entries are defined so that the sum of entries in each row is zero, i.e.,

$$L_{ii} = -\sum_{j \neq i} L_{ij}. \tag{2}$$

D. Wales [29, 30, 31] proposed to model the low temperature dynamics of a molecular cluster by the dynamics of the corresponding stochastic network. Wales and his group developed efficient tools for generating and exploring stochastic networks representing energy landscapes. A large collection of them can be found at the web site [33]. Wales's stochastic networks are complex and fascinating. They exhibit metastability, offer rich families of possible transition paths, and involve a remarkable interplay between energetic and entropic barriers. Their study evokes new theoretical paradigms and inspires the development of new computational tools.

Another context where networks with pairwise transition rates of the form of Eq. (1) arise is the evolutionary genetics. The networks represent fitness landscapes in the models of evolutionary dynamics [24, 23, 20, 13].

Analysis of large stochastic networks is an interesting and challenging problem. The number of states in the network representing an energy landscape coming from chemical physics is of the order of 10^p, $p = 3, 4, 5, 6, \ldots$. The incidence matrix is sparse but unstructured. The pairwise rates vary by tens of orders of magnitude. Therefore, it is important to develop efficient computational tools able to cope with these difficulties.

One of the most appealing analysis tools of stochastic networks is the spectral decomposition of its generator matrix. It reveals the whole collection of transition processes taking place in the system. Originally, the asymptotics for the eigenvalues for of the generator matrices with entries of the order of $e^{-U_{ij}/T}$, without the assumption of the detailed balance, was established by A. Wentzell [38, 39, 16] in 1970s. Wentzell's formulas, involing optimization among the so called W-graphs, determine the whole collection of the eigenvalues up to the exponential order.

In 2000s, Bovier and collaborators considered systems with detailed balance and assumed the presence of a spectral gap. They proved sharp estimates for low lying eigenvalues and the corresponding eigenvectors of Markov chains with detailed balance in terms of capacities and exit times, and proposed a definition of metastability in terms of metastable points (representative points for metastable sets) [3, 4, 5, 6].

Spectral analysis in the context of molecular systems was considered by Schuette and collaborators [28, 19], and another definition of metastability related to ergodicity was proposed. An application of spectral analysis to clustering can be found in [27].

In this work, we focus on the construction of an efficient algorithm for computing the complete asymptotic spectrum. Our starting point is Wentzell's formulas. We prove that in the case of detailed balance, the collection of the so called optimal

[1]This criterion for the states being connected by an edge can be relaxed. More generally, we connect states i and j by an edge (i, j) if and only if one can find a Minimum Energy Path $\phi_{ij}(\alpha)$, $\alpha \in [0, 1]$ with the following properties: (i) $\phi_{ij}(0) = x_1$ and $\phi_{ij}(1) = x_j$, where x_i and x_j are the local minima corresponding to the states i and j; (ii) ϕ_{ij} passes through no other local minima other than its endpoints x_i and x_j; (iii) the only critical points that ϕ_{ij} passes through are saddles; (iv) the maximal value of the potential along ϕ_{ij} is achieved at a Morse index one saddle. Then the number V_{ij} is the maximal potential value along ϕ_{ij}. A number of interesting phenomena regarding the Minimum Energy Paths is discussed in [8].

W-graphs in Wentzell's formulas is nested and hence can be built recursively starting from a certain minimal spanning tree and removing edges from it in a certain order. Then the exponents determining the asymptotics of eigenvalues as well the asymptotics for eigenvectors are readily found from the optimal W-graphs. These exponents also define exit rates from certain Freidlin's cycles [15, 17, 16, 7] which are easily extracted from the optimal W-graphs as well. We propose a fast computational procedure for finding the collection of the optimal W-graphs and the asymptotics for the full set of the eigenpairs starting from the smallest eigenvalues in the absolute value. Precisely, the output of the algorithm is the collection of potential differences Δ_k and sets S_k such that the eigenvalues λ_k are logarithmically equivalent to $\exp(-\Delta_k/T)$ and the eigenvectors ϕ_k are approximated by the indicator functions for the sets S_k. Modifying the stopping criterion, one can stop this algorithm as soon as the eigenvalues exceed some provided threshold.

Using our algorithm, we compute the asymptotic spectrum of Wales's stochastic network representing the Lennard-Jones cluster of 38 atoms (we will refer to it as LJ_{38}). The largest connected component of this network publicallly available via Wales's group web site [32] contains 71887 states and 119853 edges. The LJ_{38} cluster is interesting because its potential energy landscape has a double-funnel structure [12, 31]. The deeper and narrower funnel has the face-centered cubic truncated octahedron (FCC), the global minimum, at the bottom, while the shallower and wider funnel of icosahedral packings has the second lowest minimum (ICO) at the bottom. These structures are show in Fig. 5. The double funnel feature might make us expect that the corresponding network is in some sense metastable. Our results reveal that it is so in the sense of the definition by Schuette et al [28, 19] but not so in the sense of the definition of Bovier et al [3, 4] at a reasonable range of temperatures. The reason is that this network has a large collection of local minima each of which is relatively high but separated from the ground state by an even higher barrier. As a result, the set of the potential differences Δ_k, $k = 1, \dots, n-1$, defining the exponents of the eigenvalues is relatively dense. If the numbers Δ_k are ordered so that

$$\Delta_1 \geq \Delta_2 \geq \dots \geq \Delta_{n-1},$$

(i.e., the corresponding eigenvalues are ordered according to their absolute values in the increasing order), the eigenvalue corresponding to exiting from the icosahedral funnel is buried under the number 245. The gaps between the majority of the numbers Δ_k, in particular, the gap $\Delta_{245} - \Delta_{246}$, are much smaller than the temperatures at which the LJ_{38} cluster is typically considered. Thus, one cannot define, following Bovier et al, a set of metastable points, one of which corresponds to ICO, satisfying the definition of the metastability. This means, that one cannot approximate the long-time dynamics of the LJ_{38} network by defining some number $m \ll n = 71887$ of metastable sets and considering transitions between them. On the other hand, there is a large gap between the number Δ_{245}, determining the exit rate from the icosahedral basin, and the next largest Δ_k corresponding to a transition process within it. This means that if the system gets to the icosahedral basin, it will equilibrate there prior to exiting it. Therefore, the icosahedral basin is metastable in the sense of the definition by Schuette et al [28, 19].

We also would like to point out our use of disconnectivity graphs as a visualization tool. Originally, they were introduced by Becker and Karplus [2] and extensively used by Wales et al [35, 36, 31]. Traditionally, the states are arranged along the x-axis arbitrarily, just so that the graph looks aesthetical. We propose to organize

the states along the x-axis according to some ordering of interest. In particular, this ordering can be by the number of the corresponding eigenvalue. In [9], where the transition process between FCC and ICO was analyzed at finite temperature, we ordered states along the x-axis according to the committor (a. k. a. the capacitor).

The rest of the paper is organized as follows. In Section 2, we provide a brief overview of some important properties of networks with detailed balance. The theoretical relationships between the optimal W-graphs, Freidlin's cycles and the asymptotics of the spectrum are discussed in Section 3. The algorithm for computing the asymptotics of the spectrum is introduced in Section 4. The application to the LJ_{38} network is presented in Section 5. We finish this paper with a conclusion in Section 6.

2. Spectral properties of networks with detailed balance.

We consider an irreducible network with a finite set of states S and the generator matrix L given by Eqs. (1)-(2). Eqs. (1)-(2) imply that the network possesses the detailed balance property

$$\pi_i L_{ij} = \pi_j L_{ji}, \tag{3}$$

where $\pi \equiv \{\pi_1, \pi_2, \dots \pi_n\}$ is the equilibrium probability distribution satisfying

$$\pi^T L = 0, \quad \sum_{i \in S} \pi_i = 1.$$

The detailed balance condition (3) means that the expected numbers of transitions from state i to state j and vice versa per unit time are equal.

The detailed balance property dramatically simplifies the spectral analysis of the stochastic network. First, Eq. (3) implies that the generator matrix L can be decomposed as

$$L = P^{-1} Q, \tag{4}$$

where $P = diag\{\pi_1, \pi_2, \dots, \pi_n\}$, and Q is symmetric. Second, the eigenvalues of L are real and nonpositive, and the eigenvectors of L are orthogonal with respect to the inner P product. These facts can be deduced from the similarity of $L = P^{-1}Q$ and the symmetric matrix $P^{-1/2} Q P^{-1/2}$, and the strict diagonal dominance of the matrix $(tI - L)$ for any $t > 0$. The irreducibility of L implies that the eigenvalue 0 is simple. We will write the matrix of eigenvalues of L as

$$\Lambda := diag\{0, -\lambda_1, -\lambda_2, \dots, -\lambda_{n-1}\}, \quad \text{where} \quad 0 < \lambda_1 \le \lambda_2 \le \ldots \le \lambda_{n-1}. \tag{5}$$

Third, the eigen-decompositions of the matrices L and L^T can be written as

$$L = \Phi \Lambda \Phi^T P, \quad L^T = P \Phi \Lambda \Phi^T. \tag{6}$$

In particular, since the row sums of L are zeros, the eigenvector corresponding to the zero eigenvalue can be chosen to be $e := [1, 1, \dots, 1]^T$. The corresponding eigenvector of L^T is $Pe \equiv \pi$, the equilibrium probability distribution.

The spectral decomposition of the stochastic network with detailed balance leads to a nice representation of the time evolution of the probability distribution. The probability distribution evolves according to the forward Kolmogorov (a. k. a. the Fokker-Planck) equation

$$\frac{dp}{dt} = L^T p, \quad p(0) = p_0. \tag{7}$$

Using Eqs. (5) and (6) one can write the solution of Eq. (7) in the form

$$p(t) = e^{tL^T} p_0 = P\Phi e^{t\Lambda}\Phi^T p_0 = \pi + \sum_{j=1}^{n-1} (\phi_j^T p_0) P\phi_j e^{-\lambda_j t}, \tag{8}$$

where $\Phi = [e,\ \phi_1,\ \ldots,\ \phi_{n-1}]$. Eqs. (5) and (8) show that, no matter what the initial probability distribution $p(0) = p_0$ is, it will evolve eventually toward the equilibrium distribution π. However, the components $(\phi_j^T p_0) P\phi_j e^{-\lambda_j t}$ of $p(t)$ with small decay rates λ_j can remain significant for long times, $O(\lambda_j^{-1})$. If the temperature is sufficiently small, the eigenvalues λ_j of $-L$ are logarithmically equivalent to $\exp(-\Delta_j)/T$, where Δ_j are the certain constants determined by the values V_{kl} and V_i, $i, k, l, \in S$ [38, 39, 16]. Therefore, if the temperature is small enough and all numbers Δ_k are distinct, then

$$0 < \lambda_1 \ll \lambda_2 \ll \ldots \ll \lambda_{n-1}.$$

3. **The spectrum, the minimal spanning tree, and Freidlin's cycles.** In this Section, we present a construction that allows us to calculate the asymptotics for the eigenvalues and eigenvectors starting from λ_1 and ϕ_1 using a certain minimal spanning tree. Our starting point is the result established by A. Wentzell in 1970s [38, 39] (also see [16], Chapter 6).

3.1. **Wentzell's formulas.** Wentzell's theorem [38, 39] is valid for an arbitrary irreducible stochastic network with a finite number of states, not necessarily with detailed balance, where the pairwise transition rates are logarithmically equivalent to $\exp(-U_{ij}/T)$. Being adapted for networks with detailed balance where the generator matrix is of the form (1)-(2), Wentzell's theorem reads as follows.

Theorem 3.1. *Let $\lambda_1 < \lambda_2 < \ldots < \lambda_{n-1}$ be the positive eigenvalues of $-L$ where L is the generator matrix given by Eq. (1). Let us define the numbers $V^{(k)}$ as*

$$V^{(k)} = \min_{g \in G(k)} \sum_{(i \to j) \in g} (V_{ij} - V_i)\,, \tag{9}$$

where $G(k)$ is the set of W-graphs with the set $W = W_k$ containing k states. Then for $T \to 0$ we have

$$\lambda_k \asymp e^{-(V^{(k)} - V^{(k+1)})/T}, \quad k = 1, 2, \ldots, n-1. \tag{10}$$

where the symbol $\asymp$ denotes the logarithmic equivalence.

We remind that a W-graph is defined as follows [16].

Definition 3.2. Let S be the set of states. Let $W \subseteq S$ be its subset. The states in W are called sinks. A W-graph is a directed graph defined on the set of states S and possessing the following properties:

(i)**:** Each state in $S \backslash W$ is the origin of exactly one arrow.
(ii)**:** There are no cycles in the graph.

Alternatively, (ii) can be replaced with the condition that for every state $i \in S \backslash W$ there exists a sequence of arrows leading from it to a sink $j \in W$.

Thus, a W-graph with k sinks can be constructed as follows. Pick k sinks and partition the rest of the states into k subsets so that each of them contains exactly one sink. In each subset, draw arrows to connect the sets with the sink according

to the rules in Definition 3.2. If states i and j are not connected by an edge we set $V_{ij} = \infty$.

Note that if $W = S$, the W-graph contains no edges. Hence $V^{(n)}$ in Eq. (9) is zero. Therefore, $\lambda_{n-1} \asymp V^{(n-1)}$, and the number $V^{(n-1)}$ is the smallest barrier in the network:

$$V^{(n-1)} = \min_{i,j\in S,\ i\sim j}(V_{ij} - V_i).$$

If the number of states in the system is small, one can calculate the numbers $V^{(k)}$, $k = 1, 2, \ldots, n-1$ directly using Eq. (9) and find the asymptotics for the eigenvalues using Eq. (10). However, if the number of states is large, this approach becomes infeasible.

In the next few Sections, we will derive recurrence relationships for the numbers $V^{(k)}$ for the case where the pairwise rates are of the form of Eq. (1), and dramatically simplify the calculation of the asymptotic spectrum.

3.2. **The minimum spanning tree.** In this Section, we recall the definition of the minimum spanning tree and its crucial properties (see e.g. [1]). An undirected graph is called a tree if it consists of a single connected component and contains no cycles. Let $G(S, E, C)$ be a graph with the set of states S, the set of edges E, and the cost matrix $C = \{c_{ij}\}_{i,j\in S}$. If states i and j are connected by an edge, the cost c_{ij} is finite, otherwise $c_{ij} = \infty$.

Definition 3.3. Let $G(S, E, C)$ be a connected graph. A spanning tree $\mathcal{T} = G(S, E', C)$ is a connected graph with the set of states S, the set of edges $E' \subset E$, and no cycles. The total cost of the spanning tree is defined as

$$\sigma(\mathcal{T}) := \sum_{(i,j)\in E'} c_{ij}.$$

A minimum spanning tree is a spanning tree whose total cost is minimal possible.

A minimum spanning tree has two important properties: it satisfies the cut optimality condition and the path optimality condition [1]. A cut of a graph is a partition of its set of states into two subsets. The set of edges connecting states from the different subsets is called a cut-set or also a cut. The cut optimality condition states that a spanning tree $\mathcal{T}$ is a minimum spanning tree if and only if for any edge $(i, j) \in \mathcal{T}$ $c_{ij} \le c_{kl}$ for every edge (k, l) contained in the cut obtained by removing the edge (i, j) from $\mathcal{T}$. The path optimality condition claims that a spanning tree $\mathcal{T}$ is a minimum spanning tree if and only if for every edge $(k, l) \notin \mathcal{T}$, $c_{kl} \ge c_{ij}$ belonging to the unique path $w(k, l) \subset \mathcal{T}$ connecting the states k and l.

The cut optimality condition implies that the unique path $w^*(k, l)$ in a minimum spanning tree $\mathcal{T}^*$ connecting the states k and l posesses the minimax property, i.e.,

$$\max_{(i,j)\in w^*(k,l)} c_{ij} = \min_{w(k,l)\in\mathcal{W}(k,l)} \max_{(i,j)\in w(k,l)} c_{ij}, \tag{11}$$

where $\mathcal{W}(k, l)$ is the set of all paths in $G(S, E, C)$ connecting k and l. We will call a path $w^*(a, b)$ connecting a pair of states a and b minimax if for any two states $k, l \in w^*(a, b)$ the path $w^*(k, l) \subset w^*(a, b)$ satisfies Eq. (11).

A minimum spanning tree does not need to be unique. If it is unique, then for each pair of states k and l there is a unique minimax path.

For a network with pairwise rates given by Eq. (1) we define the cost $c_{ij} = V_{ij}$. This means that if the set of states of the network is equivalent to the set of local minima of a potential energy landscape, and the edges correspond to the saddles

separating the local minima, the cost of the edge (i, j) is the value of the potential at the saddle separating local minima i and j.

For the rest of the paper, we will make the following genericness assumption.

Assumption 1. *The values of the potential at the states V_i, $i \in S$, and at the edges V_{ij}, $i, j \in S$, are all different. Furthermore, all of the differences $V_{ij} - V_k$, $i, j, k \in S$, are also different.*

In particular, this means that the minimum spanning tree where the cost $c_{ij} = V_{ij}$ is unique. This minimum spanning tree $\mathcal{T}^*$ is the key object for our construction. The problem of finding the minimum spanning tree is a well-studied (see e.g. [1]). There exist a numbers of efficient algorithms for doing this.

3.3. **Notations and terminology.** In order to make our presentation clear and our equations compact, we introduce the following notations.

- A directed W-graph $g_k \in G(k)$ can be converted to a forest of k trees by making all its edges undirected. We will denote this forest by $\mathcal{T}_k$. (A graph that can be decomposed into a collection of trees is called a forest.)
- We will call a W-graph in $G(k)$, at which the minimum in Eq. (9) is achieved, optimal, and denote it by g_k^*. The corresponding forest $\mathcal{T}_k^*$ will also be called optimal.
- We will denote the W-set of the optimal graph $g_k^* \in G(k)$ by W_k^*, and call it the optimal set of sinks.

3.4. **Construction of asymptotic eigenvalues using the minimum spanning tree.** In this Section, we construct the set of numbers Δ_k determining the asymptotics for the eigenvalues using the minimum spanning tree. Simultaneously, we construct a collection of subsets $S_k \subset S$ whose indicator functions give the asymptotics for the corresponding eigenvectors. We start with the observation that Eq. (9) defining the numbers $V^{(k)}$ can be rewritten as

$$V^{(k)} = \min_{g \in G(k)} \left(\sum_{(i,j) \in \mathcal{T}_k} V_{ij} - \sum_{i \in S \setminus W_k} V_i \right) = \\ = \sum_{(i,j) \in \mathcal{T}_k^*} V_{ij} + \sum_{i \in W_k^*} V_i - \sum_{i \in S} V_i, \tag{12}$$

where $g_k^* \in G(k)$ is the optimal W-graph with k sinks, and $\mathcal{T}_k^*$ and W_k^* are the corresponding optimal forest and set of sinks. Therefore, the number $V^{(k)}$ is the sum of potentials V_{ij} over the edges of the optimal forest plus the sum of potentials over the optimal sinks minus the sum of potentials over all states. The last sum in Eq. (12) is the same for all W-graphs g_k and all $k = 1, 2, \ldots, n$. At this point, we can make the folowing observation.

Observation 1. *Let t be a connected component of the optimal W-graph g_k^*. The sink $s \in t$ is the state with the minimal value of the potential among all states $i \in t$, i.e., $V_s = \min_{i \in t} V_i$.*

If Observation 1 would not hold, we would be able to reduce the sum of potentials at the sinks while leaving optimal forest the same.

Unfortunately, the first two sums in Eq. (12) cannot be optimized independently. If we sort the states and the edges of the minimum spanning tree in the ascending order according to their potentials and take the first k states to be the sinks and

the first $n-k$ edges to constitute the forest, there is no guarantee that each subtree of the resulting forest contains exactly one sink. Therefore, determination of the numbers $V^{(k)}$ is a nontrivial constrained optimization problem. Below we propose a solution to it exploiting the nested property of the optimal W-graphs. We claim that (i) all optimal forests $\mathcal{T}_k^*$ are subgraphs of the minimum spanning tree $\mathcal{T}^*$, and (ii) the optimal W-graphs are nested. The former together with Eq. (12) immediately implies that

$$V^{(1)} = \sum_{(i,j)\in\mathcal{T}^*} V_{ij} + \min_{i\in S} V_i - \sum_{i\in S} V_i. \tag{13}$$

The latter means that all of the sinks of the optimal W-graph g_k^* are also sinks of g_{k+1}^*, and all of the edges of the optimal forest $\mathcal{T}_{k+1}^*$ are also edges of $\mathcal{T}_k^*$:

$$W_k^* \subset W_{k+1}^*, \quad k = 1, 2, \ldots, n-1, \tag{14}$$

$$\mathcal{T}_k^* \supset \mathcal{T}_{k+1}^*, \quad k = 1, 2, \ldots, n-1. \tag{15}$$

Hence, in order to obtain the optimal W-graph g_{k+1}^* from the optimal W-graph g_k^*, one needs to add exactly one sink and remove exactly one edge. Since each subtree of the optimal forest $\mathcal{T}_{k+1}^*$ must contain exactly one sink, one needs to perform three optimal picks, the last two of which need to be done simultaneously:

- pick a subtree t of the optimal forest $\mathcal{T}_k^*$,
- split it into two subtrees by removing one edge; denote the subtree containing the sink of t by t', and the other one by t'', and
- pick a new sink in the subtree t''.

Therefore, the numbers $V^{(k)}$ satisfy the following recurrence relationships:

$$V^{(k+1)} = V^{(k)} - \max_{t\in\mathcal{T}_k^*} \max_{(p,q)\in t, i\in t''} (V_{pq} - V_i), \tag{16}$$

$$\text{where} \quad t = t' \cup t'' \cup \{(p,q)\},\ t'' \cap W_k^* = \emptyset, \quad k = 1, 2, \ldots n-1.$$

Assumption 1 guarantees that in Eq. (16), the optimal edge to remove and the optimal sink to add are unique. We will denote them by (p_k^*, q_k^*) and s_{k+1}^* respectively. The asymptotics of the eigenvalue λ_k is determined by the difference $V^{(k)} - V^{(k+1)}$ according to Theorem 3.1 [38, 39, 16]. Taking into account Eq. (12) we conclude that

$$\Delta_k := V^{(k)} - V^{(k+1)} = V_{p_k^* q_k^*} - V_{s_{k+1}^*}, \quad \lambda_k \asymp \exp(-\Delta_k/T). \tag{17}$$

In the rest of this Section we will prove our claims stated above.

First we prove that all optimal forests $\mathcal{T}_k^*$ are subgraphs of the minimum spanning tree $\mathcal{T}^*$.

Theorem 3.4. *Suppose that Assumption 1 holds. Then the optimal W-graphs $g_k^* \in G(k)$, $k = 1, \ldots, n$ are subgraphs of the minimum spanning tree $\mathcal{T}^*$.*

Proof. We will proceed from converse. Let $g_k^* \in G(k)$ be the optimal W-graph, and $\mathcal{T}_k^*$ be the corresponding optimal forest. Suppose that $\mathcal{T}_k^*$ contains an edge (p,q) that does not belong to the minimum spanning tree $\mathcal{T}^*$. Suppose the edge (p,q) belongs to a subtree t of $\mathcal{T}_k^*$. Let $w^*(p,q)$ be the unique path in the minimum spanning tree $\mathcal{T}^*$ connecting the states p and q. By the path optimality condition [1] combined with Assumption 1 we have

$$V_{pq} > \max_{(i,j)\in w^*(p,q)} V_{ij}.$$

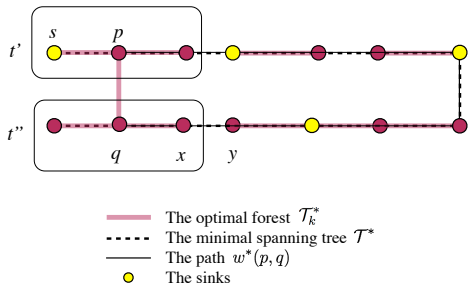

FIGURE 1. Illustration for the proof of Theorem 3.4.

The removal of the edge (p,q) splits the tree t into two subtrees t' and t'. Without the loss of the generality we assume that $p \in t'$, $q \in t''$, and the sink s of the tree t belongs to t'. Therefore, if we remove the edge (p,q) from the forest $\mathcal{T}_k^*$ and replace it with an edge $(x,y) \in w^*(p,q)$ such that $x \in t''$ and $y \notin t''$ as shown in Fig. 1, we transform the W-graph g_k^* into another W-graph $g_k^\star$ with the same set of sinks and with a smaller sum of potentials over its edges. This contradicts to the fact that g_k^* is the optimal graph. Hence the optimal W-graph g_k^* must contain only those edges that belong to the minimum spanning tree $\mathcal{T}^*$. □

Now we prove the nested property of the optimal W-graphs and the recurrence relationship for the numbers $V^{(k)}$.

Theorem 3.5. *Suppose that Assumption 1 holds. Then the optimal W-graphs are nested, i.e., Eqs. (14) and (15) hold, and the numbers $V^{(k)}$ satisfy the recurrence relationships given by Eq. (13) and (16).*

The proof of Theorem 3.5 relies on

Lemma 3.6. *Suppose that Assumption 1 holds. Then*

(*i*)**:** *the sink s_1^* of the optimal W-graph g_1^* is also a sink of the optimal W-graphs g_k^*, $k = 2, 3, \ldots, n$;*

(*ii*)**:** *the edge (p_1^*, q_1^*) that belongs to $\mathcal{T}^*$ but does not belong to $\mathcal{T}_2^*$, also does not belong to $\mathcal{T}_k^*$, $k = 3, \ldots, n$;*

(*iii*)**:** *the second sink s_2^* of the optimal W-graph g_2^* is also a sink of g_k^*, $k = 3, \ldots, n$.*

Claim (*i*) of Lemma 3.6 follows from Observation 1. Indeed, since the optimal graph g_1^* is connected, the state

$$s_1^* = \arg\min_{i \in S} V_i$$

is the sink for all optimal W-graphs g_k^*, i.e., $s_1^* \in W_k$, $k = 1, 2, \ldots, n$.

The proof of Claim (*ii*) is done from converse. The key point is to find an edge in the assumed-to-be-optimal W-graph g_k^* to be replaced with (p_1^*, q_1^*) so that the sum in Eq. (12) decreases. The choice of such an edge is different in different cases. The proof of Claim (*iii*) easily follows once Claim (*ii*) is proven. The proofs of Claims (*ii*) and (*iii*) are found in the Appendix.

Proof. (Theorem 3.5) The optimal W-graph g_1^* contains one connected component and one sink. Eq. (13) for $V^{(1)}$ immediately follows from Eq. (12) and Theorem 3.4.

The optimal W-graph g_2^* contains all edges of g_1^* except for one than we denote by (p_1^*, q_1^*), and two sinks, s_1^* (by Lemma 3.6, (i)) and s_2^*. It follows from Eq. (12) that (p_1^*, q_1^*) and s_2^* satisfy

$$\{(p_1^*, q_1^*), s_2^*\} = \arg \max_{(p,q)\in\mathcal{T}^*,\ i\in t''} (V_{pq} - V_i), \tag{18}$$

where $\mathcal{T}^* = t' \cup t'' \cup \{(p,q)\},\ s_1^* \in t'$. Therefore,

$$V^{(2)} = \sum_{(i,j)\in\mathcal{T}^*} V_{ij} - V_{p_1^* q_1^*} + V_{s_1^*} + V_{s_2^*} - \sum_{i\in S} V_i = V^{(1)} - (V_{p_1^* q_1^*} - V_{s_2^*}). \tag{19}$$

Thus, Eqs. (13)-(17) are valid for $k = 1$.

By Lemma 3.6, (ii) and (iii), the edge (p_1^*, q_1^*) does not belong to $\mathcal{T}_k^*$, $k = 3, \ldots, n$, and the sink s_2^* of the optimal W-graph g_2^* is also a sink of g_k^*, $k = 3, \ldots, n$. Therefore, we can restrict the further analysis to each of the connected components of the optimal W-graph g_2^*. Applying Lemma 3.6 to each of the connected components we obtain that (i) the sink s_2^* of the optimal W-graph g_2^* is also a sink of g_k^*, $k = 3, 4 \ldots, n$; (ii) the edge (p_2^*, q_2^*) that belongs to $\mathcal{T}_2^*$ but does not belong to $\mathcal{T}_3^*$, also does not belong to $\mathcal{T}_k^*$, $k = 4, \ldots, n$, and the third sink s_3^* of g_3^* is also a sink of g_k^*, $k = 4, \ldots, n$. Then we restrict the further analysis to each of the connected components of g_3^*. Proceeding recursively, we prove the nested property of the optimal W-graphs given by Eqs. (14) and (15). Then the recurrence relationship for the numbers $V^{(k)}$ readily follows from the nested property and Eq. (12). □

3.5. **Asymptotic eigenvectors, the optimal W-graphs, and Freidlin's cycles.** In this Section, we discuss the relationship between the asymptotic eigenvectors, the optimal W-graphs, and Freidlin's cycles. Suppose that we have constructed the optimal W-graphs g_1^*, g_2^*, ..., g_{k+1}^*. Let s_{k+1}^* be the sink of g_{k+1}^* that is not a sink of the optimal W-graphs g_1^*, g_2^*, ..., g_k^*. Let us denote by S_k the set of states in the connected component of the optimal forest $\mathcal{T}_{k+1}^*$ containing the sink s_{k+1}^*. Then it follows from the theory developed in [3] by Bovier and collaborators that the asymptotic eigenvector corresponding to the eigenvalue $\lambda_k \asymp V_{p_k^* q_k^*} - V_{s_{k+1}^*}$ is proportional to the indicator function of the set S_k. I.e., if the temperature is sufficiently small, the eigenvector corresponding to λ_k can be approximated by

$$\phi_k = [\phi_k(1), \ldots, \phi_k(n)]^T, \quad \text{where} \quad \phi_k(j) = \begin{cases} 1, & j \in S_k, \\ 0, & j \notin S_k. \end{cases} \tag{20}$$

In addition to the set of states S_k one also can consider the largest Freidlin's cycle $C_k \equiv C(s_{k+1}^*)$ containing the sink s_{k+1}^* and not containing any state with a smaller value of the potential. Below we will show that $C_k \subset S_k$. The significance of Freidlin's cycle C_k is that if the system is originally in the set S_k, it will quickly get to C_k and stay in C_k prior to exiting from the set S_k. Hence the cycle C_k can be viewed as a metastable set of states of the network in the sense that if the system is originally in C_k it will equilibrate in it prior to exiting it [28, 19]. It was proven in [3], that the eigenvalue λ_k approaches the exit rate r_k from the set S_k which is equal to the exit rate from the cycle C_k as the temperature tends to zero, i.e.,

$$\lambda_k = r_k(1 + o(1)).$$

In the rest of this Section we will clarify the claim that the asymptotic eigenvector is the indicator function for the set S_k and give an effective description of the Freidlin's cycle C_k. We will return to the discussion of metastability in Section 5.

If the temperature is small enough and Assumption 1 holds, then the eigenvalues satisfy

$$0 < \lambda_1 \ll \lambda_2 \ll \ldots \ll \lambda_{k-1} \ll \lambda_k \ll \ldots.$$

Then the normalized eigenvector ϕ_k is approximately equal to the normalized capacitor $h_{s^*_{k+1},W^*_k}$ (a.k.a. committor) [3], i.e.

$$\phi_k(j) \approx \frac{h_{s^*_{k+1},W^*_k}(j)}{\|h_{s^*_{k+1},W^*_k}\|}, \tag{21}$$

where the set W^*_k is the optimal set of sinks in the W-graph g^*_k and the capacitor $h_{s^*_{k+1},W^*_k}(j)$ is the probability that the process starting at state j first reaches state s^*_{k+1} rather then any state in the set W^*_k. The capacitor satisfies the backward Kolmogorov equation

$$\begin{cases} \sum_{i=1}^n L_{ij} h_{s^*_{k+1},W^*_k}(j) = 0, & i \notin W^*_{k+1} = W^*_k \cup \{s^*_{k+1}\}, \\ h_{s^*_{k+1},W^*_k}(i) = 0, & i \in W^*_k, \\ h_{s^*_{k+1},W^*_k}(s^*_{k+1}) = 1. \end{cases} \tag{22}$$

By our construction of the optimal W-graphs in Section 3.4, the highest potential barrier separating any state $j \in S_k$ from state s^*_{k+1} is smaller than the one separating it from any state in W^*_k, i.e.,

$$\max_{(x,y)\in w^*(j,s^*_{k+1})} V_{xy} - \min_{i\in w^*(j,s^*_{k+1})} V_i < V_{p^*_k q^*_k} - V_{s^*_{k+1}} \le \max_{(x,y)\in w^*(j,s)} V_{xy} - \min_{i\in w^*(j,s^*_{k+1})} V_i \tag{23}$$

for any $j \in S_k$ and any $s \in W^*_k$ (here $w^*(a,b)$ is the unique path in the minimum spanning tree connecting states a and b). Hence, as the temperature tends to zero, the process starting at state $j \in S_k$ will reach first s^*_{k+1} rather than any state $s \in S\backslash S_k$ with probability tending to one. On the other hand, by construction, for any state $j \in S\backslash S_k$, the highest barrier separating it from the sink in the connected component of the optimal W-graph g^*_{k+1} containing state j is strictly less than $V_{p^*_k q^*_k} - V_{s^*_{k+1}}$. Hence the probability to reach state s^*_{k+1} rather than some sink in the set W^*_k starting from state j tends to zero as temperature tends to zero. Therefore, that the capacitor $h_{s^*_{k+1},W^*_k}$ approaches the indicator function of the set S_k.

Now we remind what are Freidlin's cycles. Originally, they were introduced by M. Freidlin in 1970s in order to describe the large time behavior of systems evolving according to the SDE $dx = b(x)dt + \sqrt{2T}dw$, where $x \in \mathbb{R}^d$, $b(x)$ is a continuously differentiable vector field, and w is the Brownian motion [15]. If the parameter T is small, the dynamics of this system can be reduced to the dynamics of a continuous-time Markov chain where the states correspond to the attractors of the system [15, 17, 16].

Suppose that the vector field $b(x)$ is potential, i.e., $b(x) = -\nabla V(x)$, where $V(x)$ is twice continuously differentiable and satisfies the following conditions: (1) $V(x)$ is bounded from below, (2) $V(x)$ has n isolated local minima, (3) all saddle points of $V(x)$ have different heights, and (4) $|V(x)| \to \infty$ as $|x| \to \infty$. In this case, the long time dynamics of the system reduces to the continuous-time Markov chain with the generator of the form of Eq. (1). The hierarchy of Freidlin's cycles in this case was

studied in [7]. In particular, it was shown that the hierarchy of cycles is a full binary tree, whose leaves correspond to the potential minima or the states. They are called the zero order cycles. In total, there are $2n-1$ cycles, and there is an isomorphism between the set of Freidlin's cycles and the set of edges of the minimum spanning tree. In [15, 17, 16] the hierarchy of cycles was constructed using W-graphs. In [7] the hierarchy of cycles was constructed via a sequence of conversions of rate matrices into jump matrices and taking limits $T \to 0$. Here we will give a simple and intuitive contruction. Its justification follows from [7, 15, 17, 16].

Imagine the potential energy landscape $V(x)$, $x \in \mathbb{R}^d$, and consider the sublevel sets

$$X_a := \{x \in \mathbb{R}^d \mid V(x) < a\}, \quad a \in \mathbb{R}.$$

The sets X_a are compact. For a fixed a, either the set X_a is empty, or it consists of a finite number of connected components each of which contains at least one local minimum. The collection of local minima belonging to the same connected component of X_a forms a Freidlin's cycle. Since all saddles are assumed to have different heights (Assumption 1), each cycle consisting of more than one local minimum (i.e., of a nonzero order) can be decomposed into is a union of exactly two subcycles. This shows that the hierarchy of cycles is a complete binary tree. Suppose we are gradually increasing the level number a starting from $\min_{x\in\mathbb{R}^d} V(x)$. There will be exactly $n-1$ saddles x^* such that as a reaches $V(x^*)$, there occurs merging of two connected components of X_a that used to be disjoing for some range of smaller values of a. These $n-1$ saddles correspond to the edges of the minimum spanning tree.

Therefore, any Freidlin's cycle in the network with pairwise rates of the form of Eq. (1) can be defined as follows.

Definition 3.7. A Freidlin's cycle C containing a state $s^* \in S$ is a subset of states $C \subset S$ of the form

$$C = \left\{ s \in S \;\middle|\; \max_{(i,j)\in w^*(s^*,s)} V_{ij} < a \right\}, \tag{24}$$

where a is a constant and $w^*(s^*, s)$ is the unique path in the minimum spanning tree connecting s^* and s.

The relationship between the optimal W-graphs and the Freidlin's cycles C_k are given by

Theorem 3.8. *Suppose that Assumption 1 holds. Let s_k^* be the sink of the optimal W-graph g_k^* that is not a sink of any g_j^*, $j = 1, 2, \ldots, k-1$. Let t_k be the subtree of the optimal forest $\mathcal{T}_k^*$ containing the state s_k^*. Then the largest Freidlin's cycle C_k containing s_k^* and not containing any state s such that $V_s < V_{s_k^*}$ is the subset of states of t_k satisfying*

$$C_k = \left\{ s \in t_k \;\middle|\; \max_{(i,j)\in w^*(s_k^*,s)} V_{ij} < V_{p_{k-1}^* q_{k-1}^*} \right\}. \tag{25}$$

Proof. Let us consider the cut of the network partitioning the set of states S as

$$S = \{i \in t_k\} \cup \{i \notin t_k\}.$$

Obviously, the edge (p_{k-1}^*, q_{k-1}^*) belongs to the cut-set of this partition. We claim that the edge (p_{k-1}^*, q_{k-1}^*) has the smallest value of the potential in this partition. We proceed from converse. Suppose there is another edge (p, q) in this cut-set such that $V_{pq} < V_{p_{k-1}^* q_{k-1}^*}$. By the strong form of the cut optimality condition (see [1],

Section 13.3) (p, q) belongs to the minimum spanning tree. Let us consider the W-graph $g^{\star}_{k-1}$ that is obtained from g^{*}_{k-1} by removing the edge $(p^{*}_{k-1}, q^{*}_{k-1})$, adding the edge (p, q), and choosing the sinks properly. Let s^{*}_{a} and s^{*}_{b} be the sinks of the connected components of the optimal W-graph g^{*}_{k} adjacent to t_k via the edges $(p^{*}_{k-1}, q^{*}_{k-1})$ and (p, q) respectively (see Fig. 2). Then the corresponding sinks of

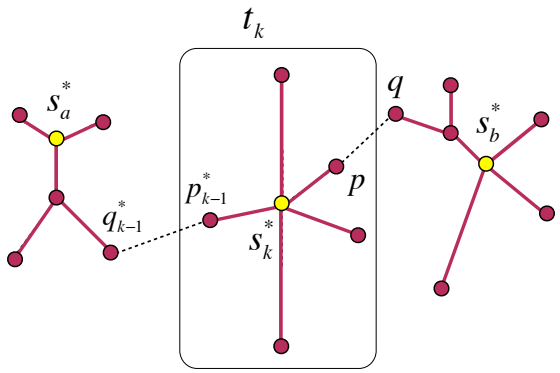

FIGURE 2. Illustration for the proof of Theorem 3.8.

the W-graph $g^{\star}_{k-1}$ are s^{*}_{a} and the one out of s^{*}_{k} and s^{*}_{b} whose potential is smaller. Since $V_{pq} < V_{p^{*}_{k-1}q^{*}_{k-1}}$ and $V_{s^{*}_{b}} \geq \min\{V_{s^{*}_{k}}, V_{s^{*}_{b}}\}$, the sum in Eq. (12) for the W-graph $g^{\star}_{k-1}$ is smaller than the one for g^{*}_{k-1}. This contradicts to the optimality of g^{*}_{k-1}. Therefore, the edge $(p^{*}_{k-1}, q^{*}_{k-1})$ has the smallest value of the potential in the cut-set, i.e.,

$$V_{p^{*}_{k-1}q^{*}_{k-1}} = \min_{p \in t_k,\ q \notin t_k} V_{pq}.$$

Therefore, the Freidlin's cycle containing s^{*}_{k} and all other states s such that

$$\max_{(i,j) \in w^{*}(s^{*}_{k}, s)} V_{ij} < V_{p^{*}_{k-1}q^{*}_{k-1}}$$

belongs to t_k, i.e., it is the cycle C_k.

Next we observe that (see Fig. 2)

$$V_{p^{*}_{k-1}q^{*}_{k-1}} = \max_{(i,j) \in w^{*}(s^{*}_{a}, s^{*}_{k})} V_{ij},$$

and this maximum is unique by Assumption 1. Hence, any larger Freidlin's cycle contains s^{*}_{a} and $V_{s^{*}_{a}} < V_{s^{*}_{k}}$. Therefore, the Freidlin's cycle C_k is the largest cycle containing s^{*}_{k} and not containing any state with a smaller value of the potential. □

4. **An algorithm for computing the asymptotic spectrum.** In this Section we propose an algorithm to compute the asymptotics for the spectrum of the generator matrix L starting from its low lying part. Central to the algorithm are the barrier function u and the escape function v defined as follows.

Definition 4.1. Let $W^{*} \subset S$ be a subset of states in the stochastic network with pairwise rates of the form (1). The barrier function $u(i)$ for the given set W^{*} is defined as

$$u(i) = \min_{s^{*} \in W^{*}} \max_{(p,q) \in w^{*}(i, s^{*})} V_{pq}, \quad i \in S, \tag{26}$$

where $w^*(s^*, i)$ is the unique path in the minimum spanning tree connecting the states s^* and i.

Definition 4.2. Let $W^* \subset S$ be a subset of states in the stochastic network with pairwise rates of the form (1). The escape function $v(i)$ for the given set of sinks W^* is defined as

$$v(i) = u(i) - V_i, \quad i \in S.$$

The output of the algorithm is the set of numbers

$$\Delta_k := V_{p_k^* q_k^*} - V_{s_{k+1}^*}$$

and the sets S_k determiniming the asymptotics of the eigenvalues and the eigenvectors respectively, and the Freidlin's cycles C_k. This Algorithm is justified by Theorems 3.4, 3.5 and 3.8.

Algorithm 1: Calculation of the asymptotic spectrum

Initialization

Precompute the minimum spanning tree $\mathcal{T}^*$. Remove all edges that do not belong to $\mathcal{T}^*$. Set

$$\begin{aligned}
&k = 0;\\
&s_1^* = \arg\min_{i \in S} V_i;\\
&u(s_1^*) = 0, \quad u(i) = \max_{(p,q) \in w^*(s_1^*, i)} V_{pq}, \quad i \in S;\\
&v(s_1^*) = 0, \quad v(i) = u(i) - V_i, \quad i \in S;\\
&\mathcal{T}_1^* = \mathcal{T}^*;\\
&S_0 \equiv C_0 = S,
\end{aligned}$$

where $w^*(s_1^*, i)$ is the unique path in $\mathcal{T}_k^*$ connecting the states s_1^* and i.

For $k = 1 : n - 1$

1. Find the new sink $s_{k+1}^* = \arg\max_{i \in S} v(i)$.
2. Find the cutting edge (p_k^*, q_k^*) in the path in $\mathcal{T}_k^*$ connecting the new sink s_{k+1}^* with one of the existing sinks:

   $$w^* = \{s_j^*, \dots, p_k^*, q_k^*, \dots, s_{k+1}^*\}, \quad j \in \{1, 2, \dots, k\},$$

   such that $u(p_k^*) < u(s_{k+1}^*)$ and $u(q_k^*) = u(s_{k+1}^*)$. Set

   $$\Delta_k = (V_{p_k^* q_k^*} - V_{s_{k+1}^*}).$$

3. Remove the cutting edge (p_k^*, q_k^*), i.e., set $\mathcal{T}_{k+1}^* = \mathcal{T}_k^* \backslash \{(p_k^*, q_k^*)\}$.
4. Set $u(s_{k+1}^*) = 0$; $v(s_{k+1}^*) = 0$.
5. Set S_k to be the collection of states in the connected component of $\mathcal{T}_k^*$ containing the sink s_{k+1}^*. For all states $i \in S_k$ update the barrier function u and the escape function v:

   $$u(i) = \min\left\{u(i), \max_{(p,q) \in w^*(s_{k+1}^*, i)} V_{pq}\right\}, \quad v(i) = \min\{v(i), u(i) - V_i\},$$

   where $w^*(s_{k+1}^*, i)$ is the unique path in $\mathcal{T}_k^*$ connecting the states s_k^* and i. The sink s_{k+1}^* and the set of states where the values of u and v have changed constitute the Freidlin's cycle C_k.

end for

There exists a collection of greedy algorithms for finding the minimum spanning tree [1]. We have used Kruskal's algorithm [21, 1] whose computational cost for a network with n states and m edges is $O(m + n \log n)$ plus the time of sorting the edges [1].

The initialization and Step 5 in the for-cycle is done using a recursive procedure in at most $n-k$ steps because the minimum spanning tree and its subgraphs contain no cycles. Step 1 in the for-cycle is done using the heap sort whose cost is $\log(n-k)$. Step 2, finding the cutting edge, requires at worst l steps if the path $w^*(s^*_{k+1}, s^*_k)$ consists of l edges. Obviously, $l \leq n-k$, and typically $l \ll n-k$.

Therefore, the upper bound for the computational cost of the for-cycle is $O(n(n-1) + n \log n - n) = O(n^2 - 2n + n \log n)$.

We remark that one can replace the for-cycle with the while-cycle in Algorithm 1 with the stopping criterion of the form $V_{p^*_k q^*_k} - V_{s^*_{k+1}} < \Delta$.

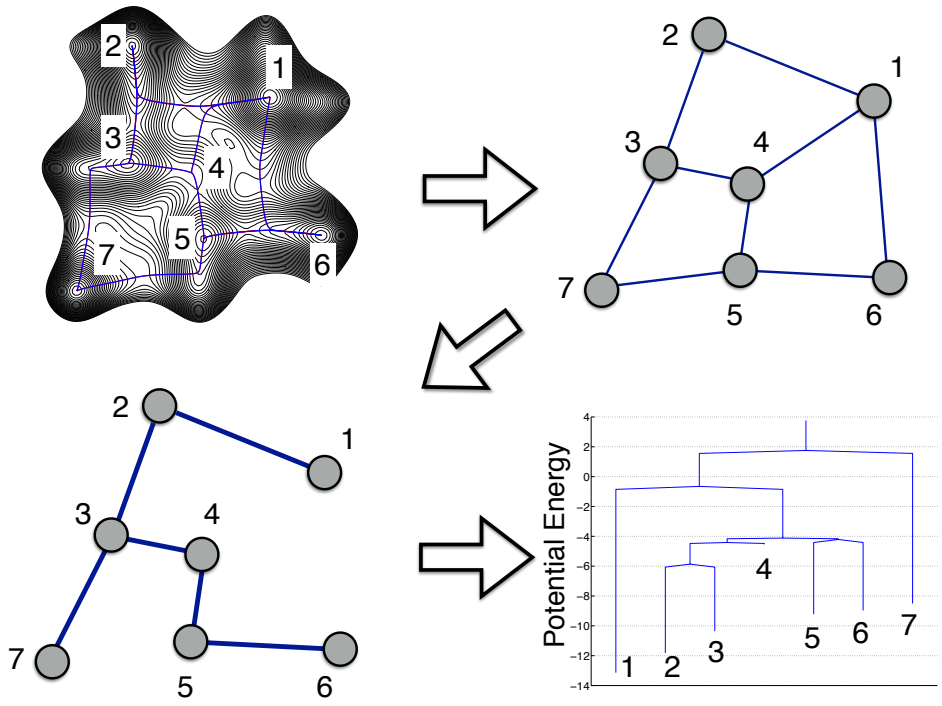

FIGURE 3. Example: the seven-well potential. The potential energy landscape is converted into a stochastic network. Then the minimum spanning tree and the disconnectivity graph are built.

We demonstrate how Algorithm 1 works on the example of the seven-well potential (Figures 3 and 4). The continuous potential energy landscape (Figure 3, top left) is converted into a stochastic network with 7 states corresponding to the potential minima (Figure 3, top right). A pair of states is connected by an edge if and only if there exists a Minimum Energy Path (MEP) connecting them that does

not pass through other minima. The resulting network contains 9 edges. The numbers V_i, $i = 1, \dots, 7$, are the values of the potential at the corresponding minima. The numbers V_{ij}, $i, j \in \{1, \dots, 7\}$, $i \neq j$, are the maximal values of the potential along the corresponding MEPs, i.e., the values of the potential at the corresponding saddles. Then we extract the minimum spanning tree (Figure 3, bottom left) that can be easily converted into the disconnectivity graph (Figure 3, bottom right).

Since state 1 corresponds to the deepest minimum, we set $s_1^* = 1$. The saddle separating minima 1 and 2 is higher than those separating minima 2, 3, 4, 5, and 6, but lower than the one separating all of them from minimum 7. The value function u and the escape function v are initialized as shown in Figure 4, top left. The set S_0 as well as Freidlin's cycle C_0 are always the whole set of states. Then the for-cycle at $k = 1$ gives the following. The maximum of v is reached at state 2. Hence state 2 becomes the new sink s_2^*. The cutting edge (p_1^*, q_1^*) is the edge $(1, 2)$. We remove it from the network. Hence the set S_1 is $\{2, 3, 4, 5, 6, 7\}$. We update the functions u and v starting the computation from state 2. State 1 does not belong to the same connected component as the new sink 2, therefore, $u(1)$ and $v(1)$ are not updated. State 7 belongs to the same connected component as state 2. However, since the highest barrier separating states 1 and 7 is the same as the one separating states 2 and 7, the values $u(7)$ and $v(7)$ remain the same. At the rest of the states, both values $u(i)$ and $v(i)$ are updated. Hence the Freidlin's cycle is $C_1 = \{2, 3, 4, 5, 6\}$ (Figure 4, top middle). Continuing in a similar manner for $k = 2, 3, \dots$, we obtain the following sequences of sinks, cutting edges, sets S_k and the corresponding Freidlin's cycles:

$$
\begin{aligned}
&s_1^* = 1, \quad S_0 = C_0 = \{1, 2, 3, 4, 5, 6, 7\},\\
&s_2^* = 2, \quad (p_1^*, q_1^*) = (1, 2), \quad S_1 = \{2, 3, 4, 5, 6, 7\}, \quad C_1 = \{2, 3, 4, 5, 6\},\\
&s_3^* = 7, \quad (p_2^*, q_2^*) = (3, 7), \quad S_2 = C_2 = \{7\},\\
&s_4^* = 5, \quad (p_3^*, q_3^*) = (4, 5), \quad S_3 = C_3 = \{5, 6\},\\
&s_5^* = 6, \quad (p_4^*, q_4^*) = (5, 6), \quad S_4 = C_4 = \{6\},\\
&s_6^* = 3, \quad (p_5^*, q_5^*) = (2, 3), \quad S_5 = \{3, 4\}, \quad C_5 = \{3\},\\
&s_7^* = 4, \quad (p_6^*, q_6^*) = (3, 4), \quad S_6 = C_6 = \{4\}.
\end{aligned}
$$

These sequences define the asymptotic eigenvalues and eigenvectors:

$$
\begin{aligned}
&\lambda_0 = 0, \quad \phi_0 = [1, 1, 1, 1, 1, 1, 1]^T,\\
&\lambda_1 \asymp \exp(-(V_{12} - V_2)/T), \quad \phi_1 = [0, 1, 1, 1, 1, 1, 1]^T,\\
&\lambda_2 \asymp \exp(-(V_{37} - V_7)/T), \quad \phi_2 = [0, 0, 0, 0, 0, 0, 1]^T,\\
&\lambda_3 \asymp \exp(-(V_{45} - V_5)/T), \quad \phi_3 = [0, 0, 0, 0, 1, 1, 0]^T,\\
&\lambda_4 \asymp \exp(-(V_{56} - V_6)/T), \quad \phi_4 = [0, 0, 0, 0, 0, 1, 0]^T,\\
&\lambda_5 \asymp \exp(-(V_{23} - V_3)/T), \quad \phi_5 = [0, 0, 1, 1, 0, 0, 0]^T,\\
&\lambda_6 \asymp \exp(-(V_{34} - V_4)/T), \quad \phi_6 = [0, 0, 0, 1, 0, 0, 0]^T.
\end{aligned}
$$

5. **Application to the Lennard-Jones-38 network.** The potential energy of a Lennard-Jones cluster LJ_N is given by

$$
V(\mathbf{r}) = 4\epsilon \sum_{i<j} \left[\left(\frac{\sigma}{r_{ij}} \right)^{12} - \left(\frac{\sigma}{r_{ij}} \right)^{6} \right], \tag{27}
$$

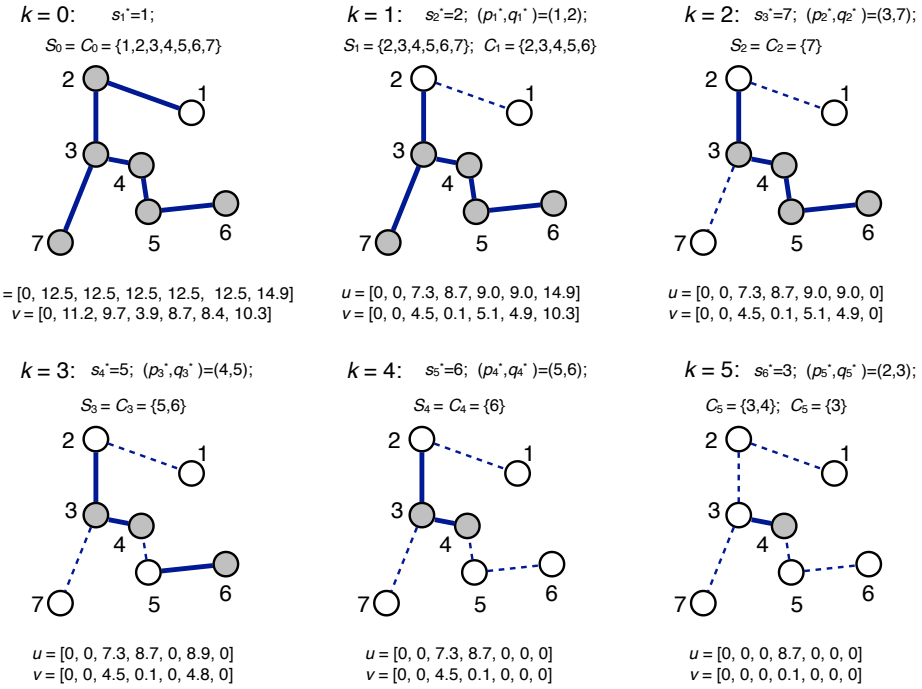

FIGURE 4. Example: the application of Algorithm 1 to the stochastic network in Figure 3. The functions u and v are computed and then updates at every step. The sequences of the sinks s_j^*, the cutting edges (p_j^*, q_j^*), and the corresponding Freidlin's cycles C_j are built in the process.

where the numbers $r_{ij} = |\mathbf{r}_i - \mathbf{r}_j|$ are the pairwize distances between the atoms. Throughout this work we will use reduced units with $k_B = \epsilon = \sigma = 1$. The majority of global potential energy minima for Lennard-Jones clusters of various sizes are based on the icosahedral packing. However, for some special numbers of atoms, Lennard-Jones clusters may admit a high symmetry configuration based on other packings [34, 12, 31]. The smallest special number is 38. The potential energy minimum of the LJ_{38} cluster is achieved at the face-centered cubic truncated octahedron with the point group O_h (Fig. 5). The second lowest minimum is the icosahedral structure with the C_{5v} point group (Fig. 5). For brevity we will refer to these configurations as FCC and ICO respectively. These two lowest minima are far disconnected in the configurational space. It was shown by Frank in 1950s [14] that as a monoatomic liquid cools, structures based on the icosahedral packing tend to appear. However, in order to crystalize, the atoms should rearrange into a periodically-extendable structure, e.g., face-centered cubic.

Wales and collaborators developed an efficient technique for conversion of potential energy landscapes into stochastic networks whose states and edges correspond to local minima and transition states (saddles of Morse index one separating pairs of local minima) respectively [12, 31, 36]. The stochastic network associated with LJ_{38} is publicly available via Wales's group web site [32]. Its connected component containing FCC and ICO (minima 1 and 7 in Wales's list respectively) contains

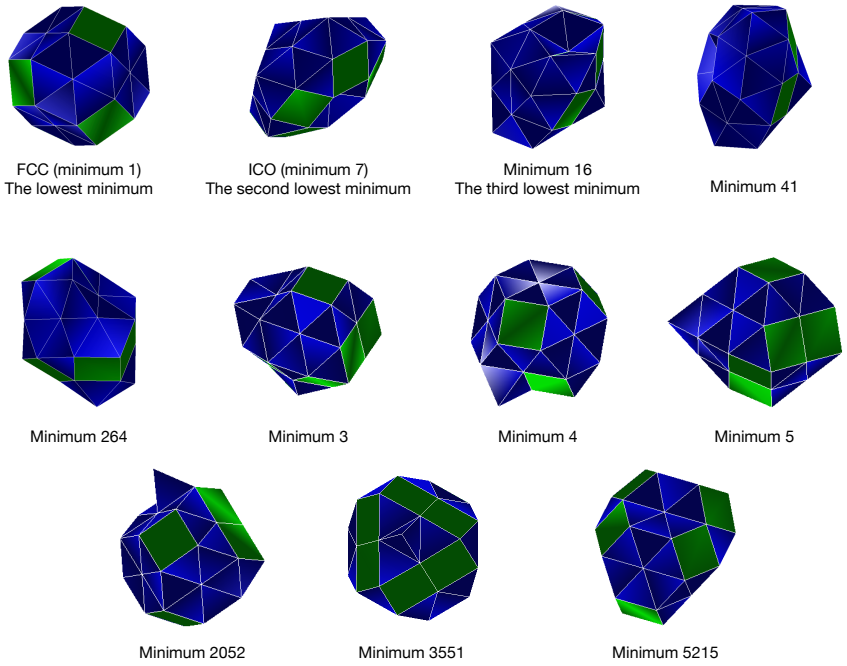

FIGURE 5. Some important local minima of the potential energy of the LJ_{38}.

71887 states and 119853 edges. We will denote the states in the LJ_{38} network other than FCC and ICO by their index in Wales's list.

The problem of the LJ_{38} cluster rearrangement has attracted a lot of attention in the past fifteen years and has become a benchmark problem in chemical physics. Many scientists attacked the problem of LJ_{38} rearrangement between its two lowest potential minima FCC and ICO using different tools. Wales analyzed the LJ_{38} network using the Discrete Path Sampling [29, 30, 31]. The asymptotic zero-temperature path connecting FCC and ICO and the sub-hierarchy of Freidlin's cycles involved into the transition process was found in [7]. A finite temperature analysis of the LJ_{38} network using the tools of the Transition Path Theory was recently conducted in [9]. The LJ_{38} cluster rearrangement in the continuous setting was also attacked by methods that do not involved the exhaustive study of the energy landscape. These methods include direct transition current sampling [26], molecular dynamics and temperature accelerated molecular dynamics [18], and parallel tempering [25].

The barrier separating FCC and ICO has the height of 4.219 and 3.543 energy units with respect to FCC and ICO respectively [12]. Typically, LJ_{38} is considered at low temperatures $0 < T \ll 1$ as the solid-solid phase transition between face-centered cubic and icosahedral structures takes place at $T = 0.12$, the outer layer starts to melt at $T = 0.18$, and the cluster melts completely at $T = 0.35$ [22]. The barrier, separating ICO from FCC is about 30 k_BT at $T = 0.12$. One might expect that the icosahedral basin with the deepest minimum ICO is, in some sense, a metastable subset of the LJ_{38} network. Our results show, however, that the situation is delicate. Whether to view the icosahedral basin as metastable or not

depends upon what definition of metastability is used and the observation time as well.

The graph of $\Delta_k := V_{p_k^* q_k^*} - V_{s_{k+1}^*}$ versus k for $k = 1, \ldots, 71886$ is shown in Fig. 6. Recall that $\lambda_k \asymp \exp(-\Delta_k/T)$. More or less notable gaps are present only between the first few barriers Δ_k corresponding to sinks with high potential evergy. These sinks are separated from the rest of the states by very high potential barriers. The eigenvalue corresponding to the sink ICO is λ_{245}. There is no significant gap separating Δ_{245}: $\Delta_{246} - \Delta_{245} \approx 0.0036$. This means that $\lambda_{245} \ll \lambda_{246}$ only for extremely low temperatures (at least, T should be less than 0.0036). The

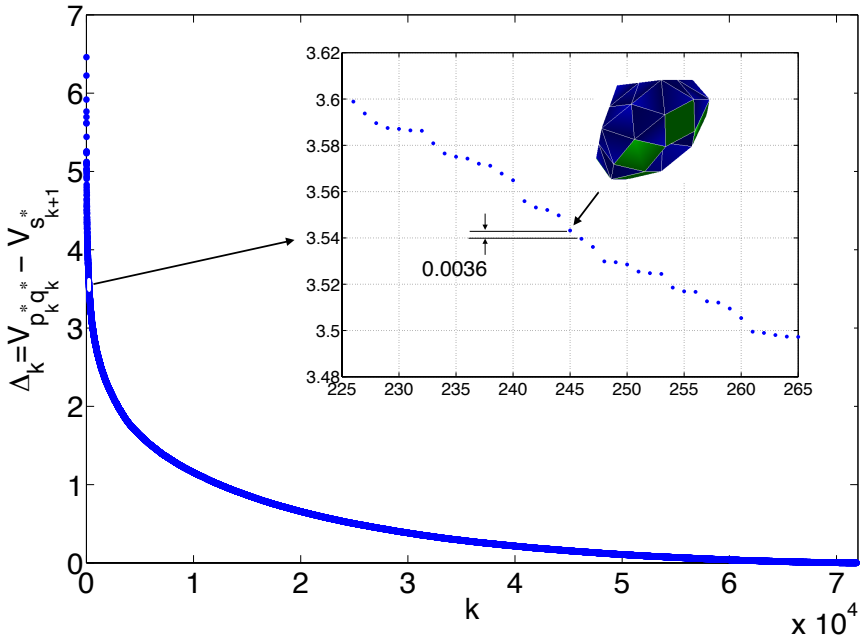

(a)

FIGURE 6. The numbers $\Delta_k := V_{p_{k-1}^* q_{k-1}^*} - V_{s_k^*}$ versus k for the LJ_{38} network.

disconnectivity graph for the sinks from s_1^* ≡FCC up to s_{300}^* is shown in Fig. 7. ICO is the sink s_{246}^*. This graph shows that if the system is initially at ICO or FCC, it is extremely unlikely for it to get to any other sink out of the first 300, if the temperature $T < 0.1$. Therefore, the sinks corresponding to the smallest eigenvalues are essentially irrelevant to the low-temperature dynamics. This means that if the system is initially not in one of these states, and the observation time is not extremely long, it is unlikely for the system to reach those states. A relevant discussion can be found in [37].

Algorithm 1 also gives the collection of sets S_k determining the asymptotic eigenvectors, and the corresponding Freidlin's cycles C_k. A few largest disjoint sets S_k, $k \geq 1$, are shown in Fig. 8. The largest set S_k for $k \geq 1$ is S_{245}, the one which appears when the sink corresponding to the second lowest minimum ICO is added. It consists of 56290 states. Freidlin's cycle C(ICO) contains 791 states. This means

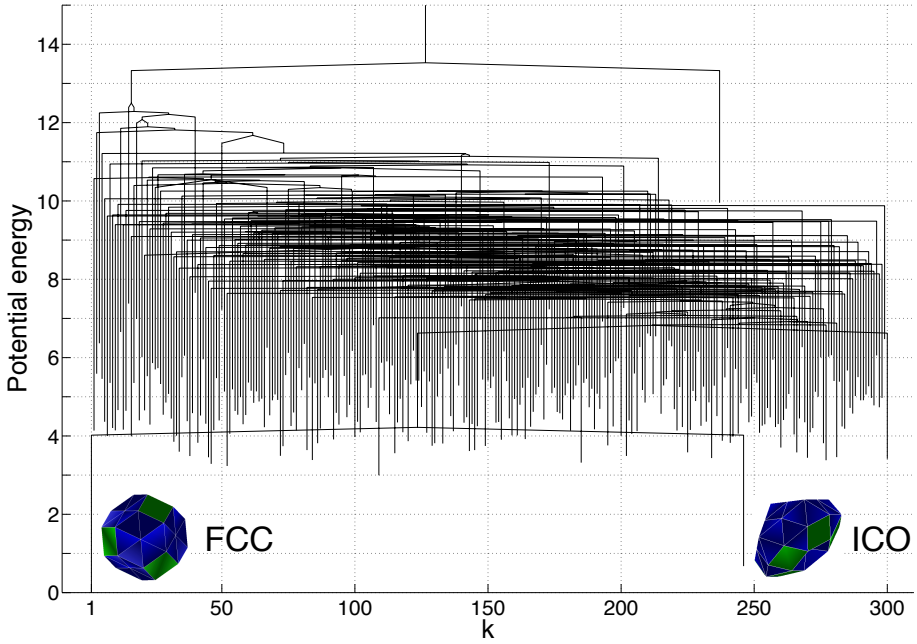

FIGURE 7. The disconnectivity graph showing the first 300 sinks of the LJ_{38} network. FCC and ICO correspond to sinks 1 and 246 respectively. The states are ordered according to the number of sink that they represent. The potential energy is shown relative to FCC.

that if the temperature is low enough and the system is initially at any state belonging to S_{245}, it relatively quickly gets to $C(\text{ICO}) \subset S_{245}$ and stays there for relatively long time $O(\exp(\Delta_{245}/T))$ prior to exiting it. The other large disjoint sets S_k, $k \geq 1$, are S_{6910} with 4252 states, the corresponding sink is minimum 3, and the corresponding Freidlin's cycle contains 3 states; S_{7482} with 1316 states, corresponding to minimum 4, and $|C(4)| = 1$; S_{5296} with 379 states, corresponding to minimum 5, and $|C(5)| = 2$; S_{4143} with 990 states, corresponding to minimum 5215, and $|C(5215)| = 8$; S_{11750} with 680 states, corresponding to minimum 3551, and $|C(3551)| = 7$; and S_{11961} with 1758 states, corresponding to minimum 2052, and $|C(2052)| = 4$. The relationship between these sets outlined in Fig. 8 is obtained using the algorithm for computing the asymptotic zero-temperature path introduced in [7]. Besides the states belonging to one of the shown sets S_k, there are 6221 more states (excluding FCC) in the LJ_{38} network that do not belong to any of the shown sets. The largest set S_k, $k \geq 1$ formed by these remaining 6221 states is S_{8009} with 288 states corresponding to minimum 587, and $C(587)$ consists of 2 states. The next largest disjoint sets S_k, $k \geq 1$, formed by the remaining states consist of 160, 98, 87, 79, ... states. Overall, the set of states in the LJ_{38} network can be decomposed into a disjoint union of the global minimum FCC and 2327 sets S_k. Out of them, 1395 sets consist of a single state, 406 consist of 2 states, 177 consist of 3 states, etc. The complete data about these disjoint sets S_k are found in Table 1.

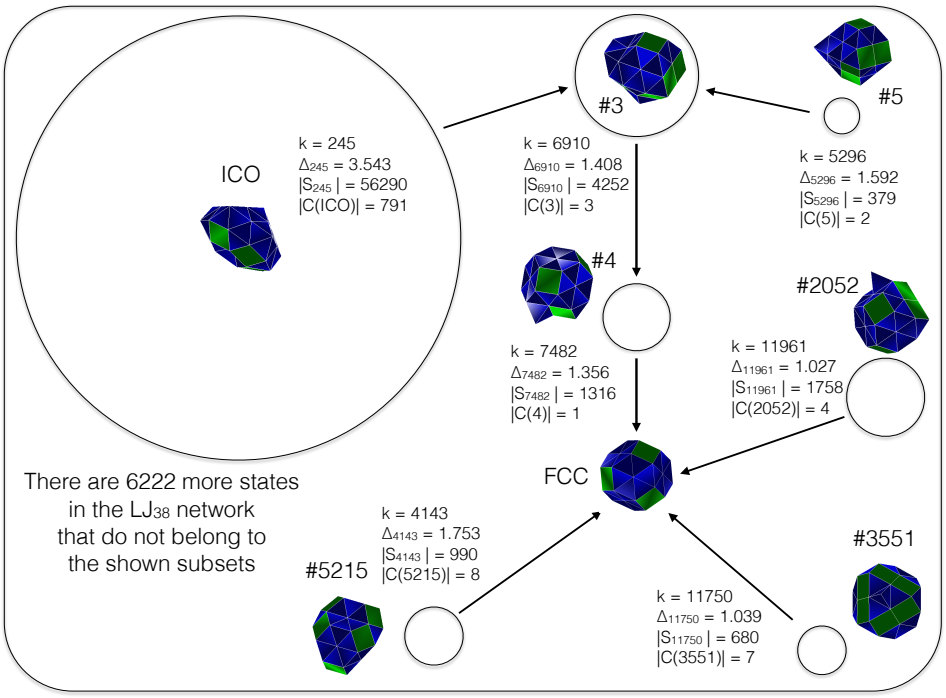

FIGURE 8. The largest disjoint sets S_k's in the LJ_{38} network together with the corresponding Δ_k's and Freidlin's cycles. The area of the circles representing the sets S_k is proportional to the number of states in them.

Fig. 7 suggests that some of the sets S_k are separated by high potential barriers from the global potential minimum FCC. This fact motivates us to restrict our attention to the part of the LJ_{38} network that is accessible from FCC at low temperatures if the observation time is large but not very large. We take the decomposition of the LJ_{38} network into the disjoint union of FCC and 2327 sets S_k and select only those S_k's that are separated from FCC by a barrier whose height does not exceed 5 relative to V_{FCC} (i.e., for these S_k's, $V_{p_k^* q_k^*} - V_{\mathrm{FCC}} < 5$ or $V_{p_k^* q_k^*} < -168.928$). All 60 such sets S_k, $k \geq 1$, are listed in Table 2. Table 2 shows that there is a significant spectral gap for the truncated and factored LJ_{38} network: $\Delta_{245} - \Delta_{4143} = 1.790$. The truncated and factored minimum spanning tree for the LJ_{38} network formed by these selected sets and FCC in Fig. 9 is calculated using the algorithm introduced in [7]. Lumping the states into disjoint sets S_k can be helpful for comparison with electron microscopy or diffraction experiments since large collection of states [32] based on icosahedral packing (395 states, states 6 through 400) is indistinguishable from low resolution experimental data. Similarly, states 1 – 5 [32] based on face-centered cubic packing are also indistinguishable. Therefore, for a careful comparison, even further lumping may be done. We leave this problem for the future.

The size distribution of Freidlin's cycles is presented in Table 3. Naturally, $C_0 \equiv C(\mathrm{FCC})$ contains all 71887 states. The second largest Freidlin's cycle is $C(\mathrm{ICO})$ containing 791 states. The third largest cycle with 45 states corresponds to the

N	The # of sets S_k with $\lvert S_k\rvert = N$	Sink(s)
56290	1	ICO
4252	1	3
1758	1	2052
1316	1	4
990	1	5215
680	1	3551
379	1	5
288	1	587
160	1	5429
98	1	2295
87	1	9087
79	1	4305
66	1	3552
54	1	7746
49	1	30562
47	1	13165
45	1	407
40	1	17251
36	1	3074
33	1	4065
28	3	45155, 77289, 85766
27	1	3191
25	3	3863, 32036, 75247
24	1	85341
23	1	6757
21	2	2, 6070
20	1	4066
18	1	11218
17	3	18648, 36425, 39076
16	4	16545, 24258, 33579, 79028
15	5	11238, 29369, 59335, 70722, 94195
14	1	9833
13	3	13287, 35221, 51978
12	10	
11	11	
10	14	
9	18	
8	21	
7	27	
6	47	
5	55	
4	97	
3	177	
2	406	
1	1395	

TABLE 1. The sizes of disjoint sets S_k constituting the set of states of the LJ_{38} network together with FCC. The indicator functions of the sets S_k are asymptotic eigenvectors.

third deepest minimum (minimum 16) (Fig. 5). Note that $C(16) \subset C(\text{ICO}) \subset S_{245}$. About 84% of Freidlin's cycles C_k consist of single states. This is the result of the fact that the states in the LJ_{38} network are separated by relatively high barriers. Therefore, one cannot significantly factor the dynamics of the LJ_{38} network by decomposing it into a disjoint union of Freidlin's cycles.

At this point, we would like to remark about the validity of Assumption 1 (the genericness assumption). Out of 71886 numbers Δ_k there are 3 repeated ones: $\Delta_{44216} = \Delta_{44217}$, $\Delta_{47405} = \Delta_{47406}$, and $\Delta_{54732} = \Delta_{54733}$. This means that special care should be taken about the corresponding asymptotic eigenvectors. However, these eigenvectors are not of interest. The rest of asymptotic eigenvectors are not affected.

k	Sink	$V_{p_k^* q_k^*}$	Δ_k	$\lvert C_k\rvert$	$\lvert S_k\rvert$
245	ICO	4.219269e+00	3.543221e+00	791	56290
4143	5215	4.171512e+00	1.753054e+00	8	990
4342	2295	4.875641e+00	1.722202e+00	4	98
4609	13165	4.837103e+00	1.683919e+00	3	47
5296	5	3.880840e+00	1.592507e+00	2	379
5804	19647	4.840889e+00	1.528352e+00	1	1
6038	5429	4.778529e+00	1.502450e+00	11	160
6521	3552	4.812691e+00	1.450600e+00	2	66
6910	3	3.763385e+00	1.408780e+00	3	4252
7482	4	3.429287e+00	1.356882e+00	1	1316
7659	9087	4.686362e+00	1.338609e+00	7	87
7675	4065	4.952008e+00	1.337357e+00	1	33
7823	407	4.864080e+00	1.325427e+00	2	45
8010	587	4.210932e+00	1.309406e+00	2	288
8231	4305	4.793179e+00	1.289844e+00	2	79
8451	26615	4.595571e+00	1.270736e+00	1	11
8498	32036	4.929577e+00	1.266567e+00	3	25
8693	55024	4.718209e+00	1.251325e+00	1	1
9464	19633	4.823696e+00	1.192426e+00	1	7
10136	12536	3.921984e+00	1.145851e+00	1	12
10833	1787	4.823821e+00	1.100551e+00	1	12
10999	43115	4.866834e+00	1.089582e+00	1	1
11355	61403	4.845165e+00	1.063956e+00	2	3
11750	3551	3.830233e+00	1.039356e+00	7	680
11961	2052	3.913145e+00	1.026976e+00	4	1758
12917	3624	4.715649e+00	9.728158e-01	2	6
14327	59098	4.457973e+00	8.977427e-01	1	1
16694	47464	4.617778e+00	7.857551e-01	2	3
19098	5074	4.788369e+00	6.897715e-01	2	9
20834	16468	4.918987e+00	6.277720e-01	1	1
22168	3190	4.871516e+00	5.837694e-01	3	3
22544	28583	4.775726e+00	5.725636e-01	2	6
24715	10735	3.882704e+00	5.094120e-01	1	1
24967	3191	3.652424e+00	5.030321e-01	1	27
25642	22585	4.686717e+00	4.854972e-01	1	1
27507	6119	4.665559e+00	4.395695e-01	1	1
27508	7135	4.779884e+00	4.395485e-01	1	3
27907	11388	4.783819e+00	4.305184e-01	1	1
29151	16976	4.575356e+00	4.012544e-01	1	2
29477	5029	3.631126e+00	3.941418e-01	1	3
31771	12970	4.339322e+00	3.465081e-01	2	2
32961	16916	4.449395e+00	3.233989e-01	1	1
34118	6129	4.579289e+00	3.027489e-01	1	1
35518	15156	4.969974e+00	2.795456e-01	1	2
38928	2	2.399623e+00	2.292819e-01	1	21
39857	5334	4.362974e+00	2.169966e-01	1	1
39872	3863	3.308673e+00	2.167377e-01	4	25
40647	3261	4.595683e+00	2.063268e-01	1	3
42847	16435	4.329995e+00	1.793789e-01	1	1
44417	7820	4.176016e+00	1.617021e-01	1	4
45846	18074	4.159332e+00	1.463683e-01	1	1
47271	26132	4.109060e+00	1.321669e-01	2	4
50106	658	4.116532e+00	1.061901e-01	1	9
54440	12347	4.885824e+00	7.330549e-02	1	1
58491	4586	4.861846e+00	4.776641e-02	1	3
59154	9102	4.999152e+00	4.385418e-02	1	1
59683	3181	4.566481e+00	4.115680e-02	1	11
61752	11817	4.893556e+00	3.039805e-02	1	1
64175	420	3.007773e+00	2.020888e-02	1	3
69069	3179	4.922959e+00	4.457720e-03	1	1

TABLE 2. The data for the truncated and factored LJ_{38} network.

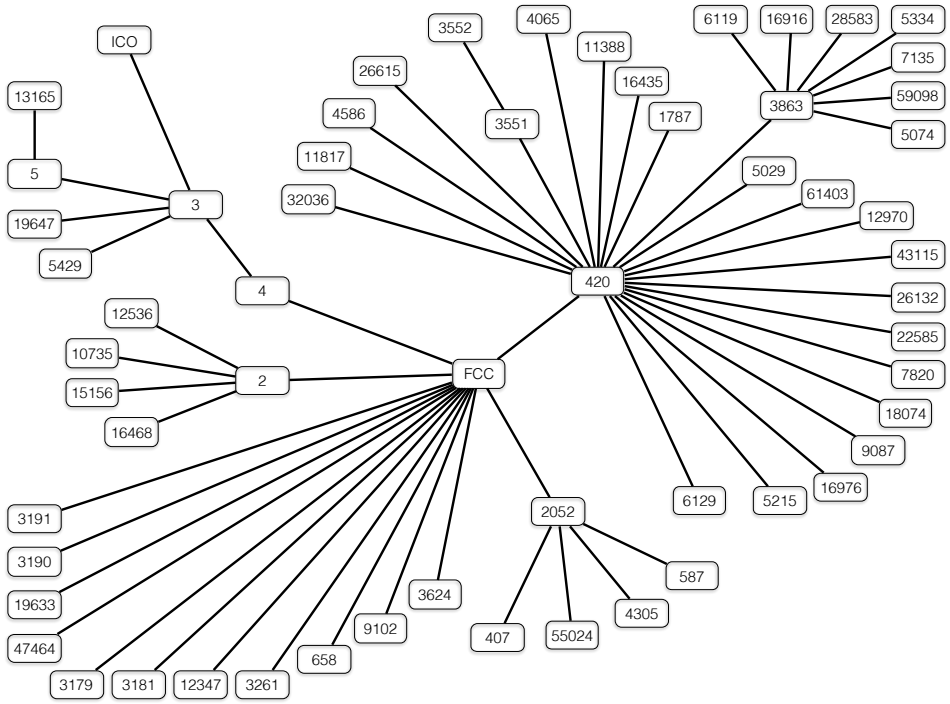

FIGURE 9. The truncated and factored minimum spanning tree for the LJ_{38} network.

N	The # of states with $\lvert C(i)\rvert = N$
71887	1
791	1
45	1
31	1
23	1
20	1
19	2
18	1
17	2
16	3
15	9
14	9
13	7
12	16
11	12
10	34
9	41
8	79
7	132
6	228
5	389
4	843
3	2108
2	6990
1	60973

TABLE 3. The distribution of sizes of Freidlin's cycles $C(i)$, $i \in S$ for the LJ_{38} network.

Now we return to the question whether the Freidlin's cycle C_{ICO} can be viewed as a metastable set at the range of temperatures $0 < T < 0.12$ (the solid-solid phase transition critical temperature is $T = 0.12$). The definition given by Bovier in [4] and adjusted to our notations and terminology sounds as follows.

Definition 5.1. A Markov process defined on a network with the set of states S is metastable with respect to the subset $\mathcal{M} \subset S$, if

$$\frac{\inf_{s\in\mathcal{M}} \mathbb{E}_s[\tau_{\mathcal{M}\setminus s}]}{\sup_{i\notin\mathcal{M}} \mathbb{E}_i[\tau_{\mathcal{M}}]} \geq \frac{1}{\rho} \gg 1, \tag{28}$$

where $\mathbb{E}_j[\tau_A]$ denotes the expected hitting time of the subset $A \subset S$ for the process starting at a state j.

The states in $\mathcal{M}$ are representative states of metastable sets. Definition 5.1 treats metastability as a way to factor the dynamics. It says that a system is metastable if one can find a subset of states $\mathcal{M}$ such that the expected time to reach from any state in $\mathcal{M}$ another state in $\mathcal{M}$ is much larger than the expected time to reach from any state not in $\mathcal{M}$ one of the states in $\mathcal{M}$. We remark that the set $\mathcal{M}$ can be chosen to be the subset of sinks $\{s_k^*\}_{k=1}^K$. In our case, if Eq. (28) holds then there exists a spectral gap

$$0 < \lambda_1 \leq \ldots \leq \lambda_{K-1} \ll \lambda_K \leq \ldots \leq \lambda_{n-1}.$$

Apparently, there is no significant spectral gap for the LJ_{38} network near λ_{245} unless $T < 0.0036$, i.e., extremely low. Therefore, the full LJ_{38} network[1] with 71887 states and infinite observation time is not metastable in the sense of the definition of Bovier and collaborators unless the temperature is extremely low.

Now let us look just at the numbers Δ_k corresponding to the states belonging to the Freidlin's cycle $C(\mathrm{ICO})$. They are plotted separately versus k in Fig. 10. The gap between $\Delta(\mathrm{ICO}) \equiv \Delta_{245}$ and the second largest Δ which is $\Delta(264) \equiv \Delta_{1379}$ is more than 1. This fact encourages us to consider the definition of metastability introduced by Schuette and collaborators in the context of general diffusion processes [28, 19]. Their definition relates metastability with ergodicity. Adjusted for stochastic networks with detailed balance it becomes

Definition 5.2. Let $s \in S$ be a state of a stochastic network with pairwise rates of the form of Eq. (1). The Freidlin's cycle $C(s)$ (the largest Freidlin's cycle containing s and not containing any state with a smaller potential value) is metastable with exit rate $\lambda(s)$ if for any state $i \in C(s)\setminus\{s\}$ the exit rate $\lambda(i)$ from the Freidlin's cycle $C(i)$ satisfies

$$\lambda(i) \gg \lambda(s). \tag{29}$$

The graph in Fig. 10 shows eloquently that the Freidlin's cycle $C(\mathrm{ICO})$ is metastable in the sense of Definition 5.2. In order to visualize the structure of the metastable state $C(\mathrm{ICO})$ we have extracted all of the sinks (ordered according to the magnitude of the corresponding eigenvalue) lying in $C(\mathrm{ICO})$ and plotted a disconnectivity graph for the fisrt 20 of them. We have also included the sink corresponding to FCC (see Fig. 11). The first four sinks in this substructure are ICO, minimum 264 in Wales's list [32], the third lowest minimum (minimum 16), and minimum 41. These four minima correspond to those eigenvalues of the reduced

[1]Actually, Wales's group created a more complete LJ_{38} network with over a million of local minima. Only its part containing the lowest 10^5 local minima is available at [32], but it is sufficient for modeling the low-temperature dynamics.

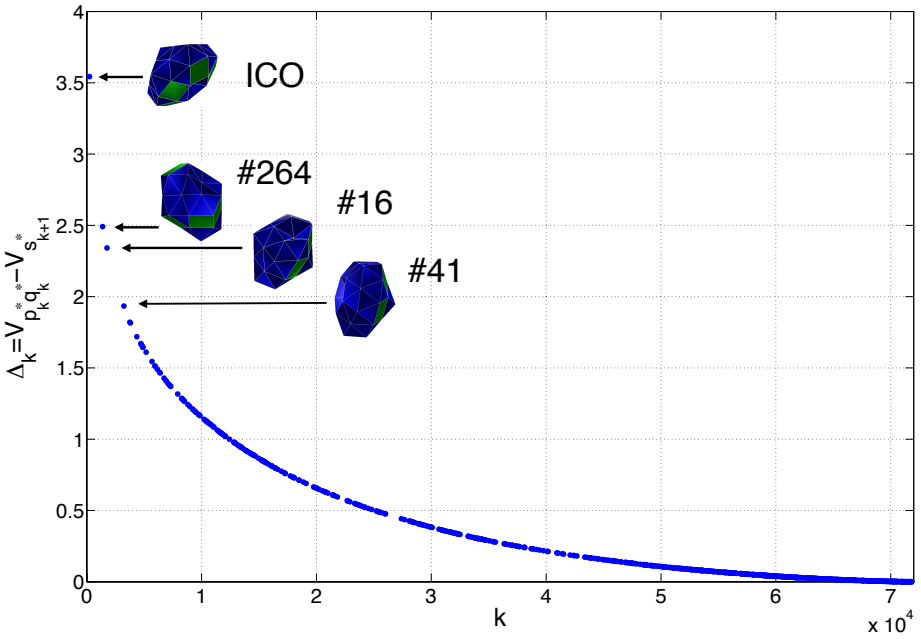

FIGURE 10. The numbers $\Delta_k := V_{p_k^* q_k^*} - V_{s_{k+1}^*}$ versus k corresponding to the states belonging to the Freidlin's cycle $C(\text{ICO})$.

LJ_{38} network separated by spectral gaps from the rest. It is apparent from the disconnectivity graph that minimum 264 is separated from ICO by almost as high barrier as the one separating ICO and FCC. Freidlin's cycle $C(264)$ consists of 4 states.

Finally, we perform one more experiment with the LJ_{38} network. Instead of lumping together states constituting disjoint sets S_k and the putting a cap on the highest admissible potential barrier, we simply truncate the LJ_{38} network without any lumping. Exactly, we remove all edges (i, j) with $V_{ij} > 6.0 + V_{\text{FCC}}$ and take the connected component of the resulting network containing FCC and ICO. It consists of 30520 states and 71750 edges. This cut off is equivalent to limiting the observation time. The graph of the first 100 Δ_k is shown in Fig. 12. There are notable gaps in Δ's. These differences are $\Delta_1 - \Delta_2 \approx 0.19$, $\Delta_2 - \Delta_3 \approx 0.46$, $\Delta_3 - \Delta_4 \approx 0.11$, and $\Delta_4 - \Delta_5 \approx 0.15$. The other differences are significanly smaller. The first eigenvalue λ_1 is smaller than λ_2 by the factor of at least 10 if the temperature $T < 0.083$. All four first eigenvalues are separated by gaps of at least of the factor of 10 if the temperature $T < 0.047$. Therefore, the truncated LJ_{38} network is metastable with respect to ICO and FCC in the sense of Definition 5.1 if $T < 0.083$. It is metastable in the sense of Definition 5.1 with respect to five metastable points, FCC, ICO, and the ones corresponding to Δ_2, Δ_3 and Δ_4 in Fig. 12 (minima 223, 21450 and 7583 in Wales's list [32]) if $T < 0.047$. The disconnectivity graph showing the first 101 sinks of the reduced LJ_{38} network is shown in Fig. 13.

6. **Conclusion.** In this work we have considered stochastic networks representing potential energy landscapes. We have established a connection between the optimal

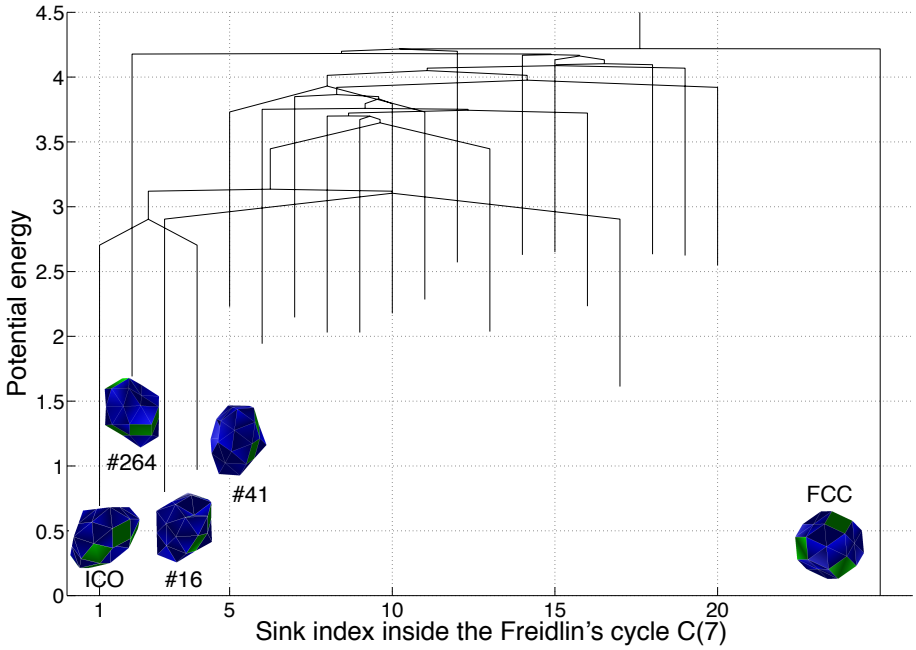

FIGURE 11. The disconnectivity graph showing the first 20 sinks belonging to the Freidlin's cycle $C(\mathrm{ICO})$. The states are ordered in the increasing order of the sink inside $C(\mathrm{ICO})$. The potential energy is shown relative to FCC.

W-graphs determining the asymptotics of the eigenvalues [38, 39, 16] and the minimum spanning tree for the edge cost equal to the potential at the corresponding saddle. We have proven the nested property of the optimal forests corresponding to the optimal W-graphs, i.e., $\mathcal{T}^*_{k+1} \subset \mathcal{T}^*_k$, $k = 1, 2, \ldots, n$, and established recurrence relationships allowing us to construct the optimal forests and calculate the asymptotics for the eigenvalues and the eigenvectors. We have reconciled Wentzell's formulas, the optimal W-graphs, Freidlin's cycles and sharp estimates for the low lying spectra by Bovier and collaborators in our construction.

Relying on our theoretical results (Theorems 3.4 -3.8), we have proposed an efficient algorithm for computing the asymptotic spectrum starting from the smallest eigenvalues in the absolute value. In the nutshell, this algorithm is a procedure for cutting the minimum spanning tree in a certain order. It is extremely robust and suitable for complex networks with large numbers of states and edges that do not have to possess any special structural properties other than the genericness assumption (Assumption 1).

We have applied this algorithm to Wales's Lennard-Jones-38 network [32]. Since the energy landscape of the LJ_{38} has a double-funnel structure, one could expect that the LJ_{38} network should have a spectral gap separating the eigenvalue corresponding to the transition from the larger and shallower icosahedral funnel to the deeper and narrower face-centered cubic funnel from the rest. However, our results demonstrate that this is not the case for the full LJ_{38} network available at [32]. The

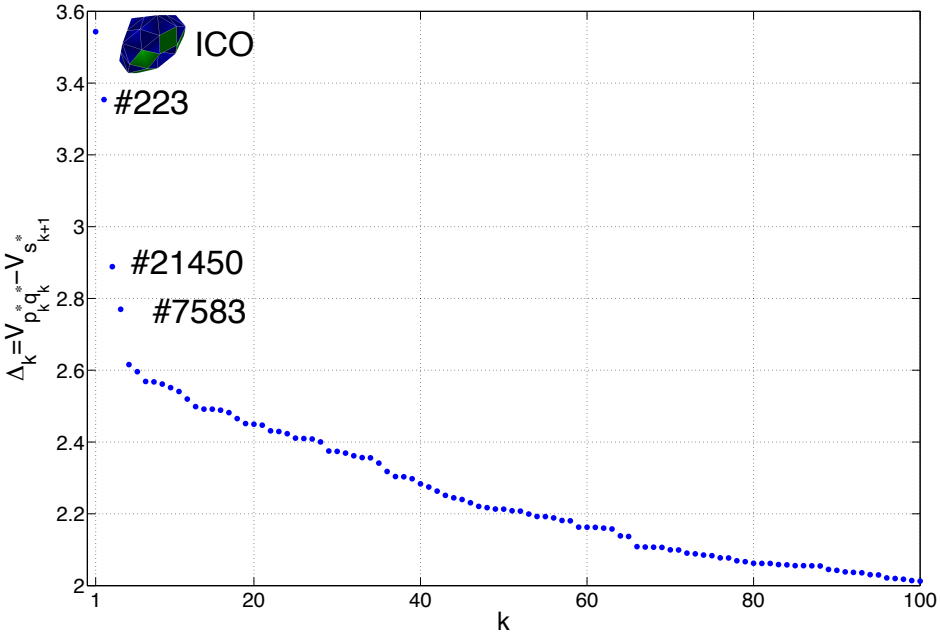

FIGURE 12. The numbers $\Delta_k := V_{p_k^* q_k^*} - V_{s_{k+1}^*}$ versus k for the reduced LJ_{38} network. Only the first 100 Δ_k's are shown.

aforementioned eigenvalue has number 245 in the ordered list and it is not separated from the rest by a notable spectral gap. On the other hand, the sinks corresponding to the smallest eigenvalues are essentially irrelevant to the low temperature dynamics. If the system is initially at the global minimum FCC, the temperature is low, and the observation time is not very large, these high-lying states will be extremely unlikely to observe during an experiment or a simulation. Putting a cap on the highest barrier separating states from FCC which is equivalent to limiting the observation time and/or lumping together sets of states, we can obtain a notable spectral gap. Furthermore, without any capping or lumping, Freidlin's cycle $C(\text{ICO})$ is metastable according to Definition 5.2 related to ergodicity.

Spectral analysis suggests a way to factor the network-in-hand. We have demonstrated how this can be done for the LJ_{38} network. The decomposition of the network into disjoint sets S_k (whose indicator functions are subset of the asymptotic eigenvectors) is helpful for simplification and visualization of low-temperature dynamics. It also might be helpful for comparison with experiment, a problem that we leave for the future.

Acknowledgments. I am grateful to Prof. E. Vanden-Eijnden for making me interested in the spectral problem and for valuable discussions. I thank Prof. M. Freidlin for a valuable discussion. I thank Prof. D. Wales for referring me to his LJ_{38} network and valuable discussion. This work is supported by the DARPA YFA Grant N66001-12-1-4220 and the NSF grant 1217118.

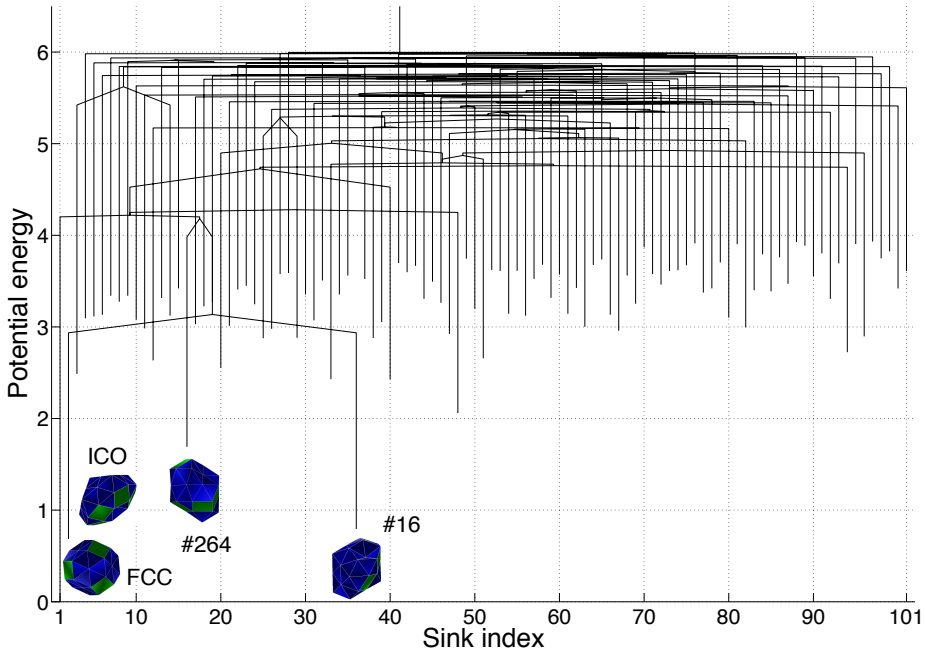

FIGURE 13. The disconnectivity graph showing the first 101 sinks of the truncated LJ_{38} network. The states are ordered according to the number of sink that they represent in the truncated network. The potential energy is shown relative to FCC.

Appendix A. Proof of Lemma 3.6.

Proof. First we prove Claim (ii). We will proceed from converse. Let us assume that the edge (p_1^*, q_1^*) belongs to the optimal graph g_k^* for some $k \in \{3, \dots, n-1\}$. Then one can replace (p_1^*, q_1^*) with another edge (p, q) not in g_k^* and possibly pick another sink so that the sum over the edges and sinks in Eq. (12) decreases. I.e., if g_k is the W-graph obtained as a result of these replacements, and $\mathcal{T}_k$ and W_k are the corresponding tree and the set of sinks of g_k, then

$$\sum_{(i,j)\in\mathcal{T}_k} V_{ij} + \sum_{i\in W_k} V_i < \sum_{(i,j)\in\mathcal{T}_k^*} V_{ij} + \sum_{i\in W_k^*} V_i.$$

There is no single recipe for the choice of the edge (p, q). We will have to consider several cases. Let $w_{12}^* := w^*(s_1^*, s_2^*)$ be the unique path in the minimum spanning tree $\mathcal{T}^*$ connecting the sinks s_1^* and s_2^* of the optimal W-graph g_2^*. The edge (p_1^*, q_1^*) must belong to w_{12}^*, as s_1^* and s_2^* belong to different connected components of g_2^*. Without the loss of generality we assume that

$$w_{12}^* = \{s_1^*,\ \dots, p_1^*,\ q_1^*,\ \dots,\ s_2^*\}.$$

We observe that

$$V_{p_1^* q_1^*} = \max_{(p,q)\in w_{12}^*} V_{pq}, \tag{30}$$

as otherwise we get a contradiction with Eq. (18). By Assumption 1 the maximum in Eq. (30) is reached at the unique edge (p_1^*, q_1^*).

Further we will need the following definition. Let us consider the W-graph $\hat{g}$ obtained from g_k^* by removing the edge (p_1^*, q_1^*) and adjusting the directions of the edges so that the sink of each connected component of $\hat{g}$ is the state with minimal potential in it. Then for any state i, $sink(i)$ is the sink of the connected component of $\hat{g}$ containing i. We will consider five cases:

Case A: All edges of the path w_{12}^* belong to g_k^*.
Case B: There is an edge in w_{12}^* not belonging to g_k^*.
  Case B.1: $V_{sink(p_1^*)} \le V_{sink(q_1^*)}$
    Case B.1.1: There is an edge $(p,q) \in w^*(q_1^*, s_2^*) \subset w_{12}^*$ such that $(p,q) \notin \mathcal{T}_k^*$.
    Case B.1.2: The whole path $w^*(q_1^*, s_2^*)$ belongs to g_k^*.
  Case B.2: $V_{sink(p_1^*)} > V_{sink(q_1^*)}$.
    Case B.2.1: There is an edge $(p,q) \in w^*(s_1^*, p_1^*) \subset w_{12}^*$ such that $(p,q) \notin \mathcal{T}_k^*$.
    Case B.2.2: The whole path $w^*(s_1^*, p_1^*)$ belongs to $\mathcal{T}_k^*$.

Cases A, B.1.1, B.1.2, and B.2.1 are illustrated in Fig. 14. Case B.2.2 is impossible. Indeed, if the whole path $w^*(s_1^*, p_1^*)$ belongs to g_k^* then the states p_1^* and s_1^* belong to the same connected component of g_k^*. Hence $sink(p_1^*) = s_1$, the state with the minimal potential in the whole network. This contradicts to the assumption that $V_{sink(p_1^*)} > V_{sink(q_1^*)}$.

Now we will explain how to choose the edge (p,q) in each of the cases A, B.1.1, B.1.2, and B.2.1.

Case A: Since the W-graph g_k^* is not connected, there is an edge $(p,q) \in \mathcal{T}^*$ such that $(p,q) \notin g_k^*$ and p belongs to the connected component of g_k^* containing the path w_{12}^* (see Fig. 14(a)). Replacing the edge (p_1^*, q_1^*) with the edge (p,q) and choosing s_2^* to be $sink(q_1^*)$, we transform the optimal W-graph g_k^* into another W-graph g_k. By the assumption that g_k^* is optimal we have

$$V_{p_1^* q_1^*} + V_{sink(q)} - (V_{pq} + V_{s_2^*}) < 0, \quad \text{i.e.} \quad V_{p_1^* q_1^*} - V_{s_2^*} < V_{pq} - V_{sink(q)}. \tag{31}$$

The inequalities above are strict by Assumption 1. This contradicts to the definition of (p_1^*, q_1^*) and s_2^* given by Eq. (18). Hence the W-graph g_k^* is not optimal.

Case B.1.1: In this case, there is an edge $(p,q) \in w^*(q_1^*, s_2^*)$ such that $(p,q) \notin g_k^*$ but $w^*(q_1^*, p) \in g_k^*$ (see Fig. 14(b), Top). Replacing the edge (p_1^*, q_1^*) with the edge (p,q) and properly choosing sinks, we transform the optimal graph g_k^* into another W-graph g_k. By the assumption that g_k^* is optimal we have

$$\begin{aligned} &V_{p_1^* q_1^*} + \min\{V_{sink(p_1^*)}, V_{sink(q_1^*)}\} + V_{sink(q)} \\ &- (V_{pq} + V_{sink(p_1^*)} + \min\{V_{sink(q_1^*)}, V_{sink(q)}\}) \le 0. \end{aligned} \tag{32}$$

By assumption, $V_{sink(p_1^*)} \le V_{sink(q_1^*)}$. Hence $\min\{V_{sink(p_1^*)}, V_{sink(q_1^*)}\} = V_{sink(p_1^*)}$. Therefore,

$$V_{p_1^* q_1^*} + V_{sink(q)} < V_{pq} + \min\{V_{sink(q_1^*)}, V_{sink(q)}\}). \tag{33}$$

The inequality above is strict by Assumption 1. Noting that $V_{sink(q)} \ge \min\{V_{sink(q_1^*)}, V_{sink(q)}\}$ we conclude that $V_{p_1^* q_1^*} < V_{pq}$. This contradicts to the fact that that $V_{p_1^* q_1^*} = \max_{(i,j) \in w_{12}^*} V_{ij}$ (see Eq. (30)). Hence g_k^* is not optimal.

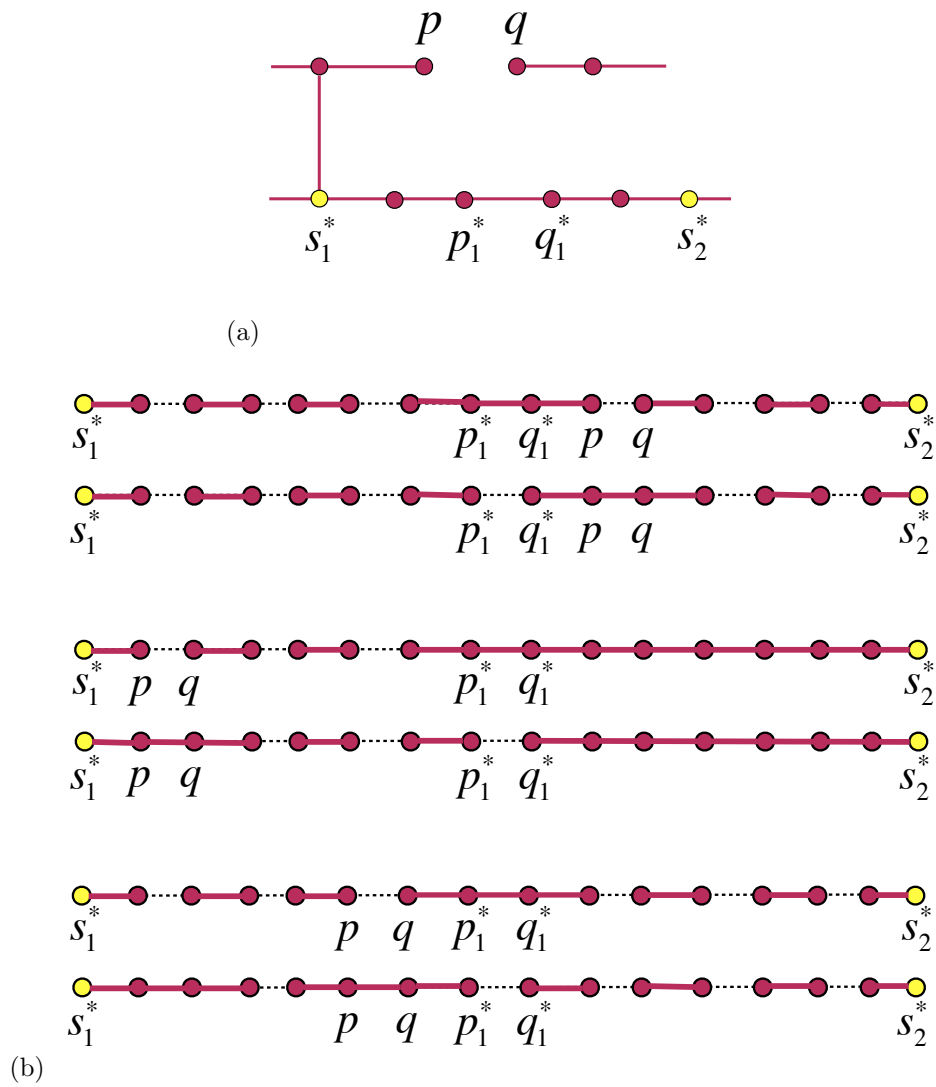

FIGURE 14. Illustration for the proof of Theorem 3.5. (a): Case A. (b): Case B. Top: Case B.1.1. Center: Case B.1.2. Bottom: Case B.2.1

Case B.1.2: In this case, there is an edge $(p, q) \in w^*(s_1^*, p_1^*)$ such that $(p, q) \notin g_k^*$ but $w(a, p) \in g_k^*$ (see Fig. 14(b), Center). Replacing the edge (p_1^*, q_1^*) with the edge (p, q) and choosing s_2^* to be $sink(q_1^*)$, we transform the optimal graph g_k^* into another W-graph g_k. By the assumption that g_k^* is optimal we have

$$V_{p_1^* q_1^*} + V_{sink(q)} + \min\{V_{sink(p_1^*)}, V_{sink(q_1^*)}\} - (V_{pq} + V_{sink(p_1^*)} + V_{s_2^*}) \leq 0. \quad (34)$$

By assumption, $V_{sink(p_1^*)} \leq V_{sink(q_1^*)}$. Hence $\min\{V_{sink(p_1^*)}, V_{sink(q_1^*)}\} = V_{sink(p_1^*)}$. Therefore,

$$V_{p_1^* q_1^*} - V_{s_2^*} < V_{pq} + V_{sink(q)}. \quad (35)$$

The inequality above is strict by Assumption 1. This contradicts to the definition of (p_1^*, q_1^*) and s_2^* given by Eq. (18). Hence g_k^* is not optimal.

Case B.2.1: In this case, there is an edge $(p,q) \in w^*(s_1^*, p_1^*)$ such that $(p,q) \notin g_k^*$ but $w^*(q, p_1^*) \in g_k^*$ (see Fig. 14(b), Bottom). Replacing the edge (p_1^*, q_1^*) with the edge (p,q) and properly choosing sinks, we transform the optimal graph g_k^* into another W-graph g_k. By the assumption that g_k^* is optimal we have

$$V_{p_1^* q_1^*} + V_{sink(p)} + \min\{V_{sink(p_1^*)}, V_{sink(q_1^*)}\} - (V_{pq} + V_{sink(q_1^*)} + \min\{V_{sink(p)}, V_{sink(p_1^*)}\}) \le 0. \tag{36}$$

By assumption, $V_{sink(p_1^*)} > V_{sink(q_1^*)}$, hence $\min\{V_{sink(p_1^*)}, V_{sink(q_1^*)}\} = V_{sink(q_1^*)}$. Therefore,

$$V_{p_1^* q_1^*} + V_{sink(p)} < V_{pq} + \min\{V_{sink(p)}, V_{sink(p_1^*)}\}. \tag{37}$$

The inequality above is strict by Assumption 1. Noting that $V_{sink(p)} \ge \min\{V_{sink(p_1^*)}, V_{sink(p)}\}$ we conclude that $V_{p_1^* q_1^*} < V_{pq}$. This contradicts to the fact that that $V_{p_1^* q_1^*} = \max_{(i,j)\in w_{12}^*} V_{ij}$ (see Eq. (30)). Hence g_k^* is not optimal.

Now we prove Claim (*iii*). Since the edge (p_1^*, q_1^*) does not belong to g_k^*, $k = 2, 3, \ldots, n$, the states s_1^* and s_2^* belong to different connected components of the graphs g_k^*, $k = 2, 3, \ldots, n$. By Observation 1, the state s_2^* has the smallest value of the potential in its connected component of g_2^*. Since the connected components of g_k^*, $k = 3, \ldots, n$ containing the state s_2^* are subgraphs of the of the connected component of g_2^* containing s_2^*, s_2^* has also the smallest value of the potential in its connected components of g_k^*, $k = 3, \ldots, n$. Therefore, it must be a sink of g_k^*, $k = 3, \ldots, n$. □

REFERENCES

[1] R. K. Ahuja, T. L. Magnanti and J. B. Orlin, *Network Flows: Theory, Algorithms, and Applications*, Prentice Hall, New Jersey, 1993.

[2] O. M. Becker and M. Karplus, The topology of multidimensional potential energy surfaces: theory and application to peptide structure and kinetics, *J. Chem. Phys.*, **106** (1997), 1495–1517.

[3] A. Bovier, M. Eckhoff, V. Gayrard and M. Klein, Metastability and low lying spectra in reversible Markov chains, *Comm. Math. Phys.*, **228** (2002), 219–255.

[4] A. Bovier, Metastability, in *Methods of Contemporary Statistical Mechanics*, (ed. R. Kotecky), Lecture Notes in Math., Springer, **1970** (2009), 177–221.

[5] A. Bovier, M. Eckhoff, V. Gayrard and M. Klein, Metastability in reversible diffusion processes I. Sharp estimates for capacities and exit times, *J. Eur. Math. Soc.*, **6** (2004), 399–424.

[6] A. Bovier, V. Gayrard and M. Klein, Metastability in reversible diffusion processes. II. Precise estimates for small eigenvalues, *J. Eur. Math. Soc.*, **7** (2005), 69–99.

[7] M. K. Cameron, Computing Freidlin's cycles for the overdamped Langevin dynamics, *J. Stat. Phys.*, **152** (2013), 493–518.

[8] M. Cameron, R. V. Kohn, and E. Vanden-Eijnden, The string method as a dynamical dystem, *J. Nonlin. Sc.*, **21** (2011), 193–230.

[9] M. K. Cameron and E. Vanden-Eijnden, Flows in complex networks: Theory, algorithms, and application to Lennard-Jones cluster rearrangement, *J. Stat. Phys.*, **156** (2014),427–454. arXiv:1402.1736.

[10] J. W. Demmel, *Applied Numerical Linear Algebra*, SIAM, 1997.

[11] E. W. Dijkstra, A note on two problems in connexion with graphs, *Numerische Mathematic*, **1** (1959), 269–271.

[12] J. P. K. Doye, M. A. Miller and D. J. Wales, The double-funnel energy landscape of the 38-atom Lennard-Jones cluster, *J. Chem. Phys.*, **110** (1999), 6896–6906.

[13] W. J. Ewens, *Mathematical Population Genetics 1: Theoretical Introduction*, 2nd Ed., Springer Science+Business Media, Inc., 2004.

[14] F. C. Frank, Supercooling of liquids, *Proc. R. Soc. Lond. A Math. Phys. Sci.*, **215** (1952), 43–46.

[15] M. I. Freidlin, Sublimiting distributions and stabilization of solutions of parabolic equations with small parameter, *Soviet Math. Dokl.*, **18** (1977), 1114–1118.

[16] M. I. Freidlin and A. D. Wentzell, *Random Perturbations of Dynamical Systems*, 3rd ed, Springer-Verlag Berlin Heidelberg, 2012.

[17] M. I. Freidlin, Quasi-deterministic approximation, metastability and stochastic resonance, *Physica D*, **137** (2000), 333–352.

[18] J. C. Hamilton, D. J. Siegel, B. P. Uberuaga and A. F. Voter, Isometrization rates and mechanisms for the 38-atom Lennard-Jones cluster determined using molecular dynamics and temperature accelerated molecular dynamics, preprint.

[19] W. Huisinga, S. Meyn and Ch. Schuette, Phase transitions and metastability in Markovian and molecular systems, *Ann. Appl. Prob.*, **14** (2004), 419–458.

[20] M. Kimura, *The Neutral Theory of Molecular Evolution*, Cambridge University Press, 1985.

[21] J. B. Kruskal, On the shortest spanning subtree of a graph and the traveling salesman problem, *Proc. Amer. Math. Soc.*, **7** (1956), 48–50.

[22] V. A. Mandelshtam and P. A. Frantsuzov, Multiple structural transformations in Lennard-Jones clusters: Generic versus size-specific behavior, *J. Chem. Phys.*, **124** (2006), 204511.

[23] J. H. Gillespie, *Population Genetics: A Concise Guide*, 2nd Ed. John Hopkins University Press, 2004.

[24] M. Manhart and A. V. Morozov, Statistical Physics of Evolutionary Trajectories on Fitness Landscapes, preprint, `arXiv:1305.1352`.

[25] J. P. Neirotti, F. Calvo, D. L. Freeman and J. D. Doll, Phase changes in 38-atom Lennard-Jones clusters. I. A parallel tempering study in the canonical ensemble, *J. Chem. Phys.*, **112** (2000), 10340.

[26] M. Picciani, M. Athenes, J. Kurchan and J. Taileur, Simulating structural transitions by direct transition current sampling: the example of LJ_{38}, *J. Chem. Phys.*, **135** (2011), 034108.

[27] M. Sarich, N. Djurdjevac, S. Bruckner, T. O. F. Conrad and Ch. Schuette, Modularity revisited: a novel dynamics-based concept for decomposing complex networks, *Journal of Computational Dynamics*, (2013) (In Press).

[28] Ch. Schuette, W. Huisinga and S. Meyn, Metastability of diffusion processes, *IUTAM Symposium on Nonlinear Stochastic Dynamics Solid Mechanics and Its Applications*, **110** (2003), 71–81.

[29] D. J. Wales, Discrete Path Sampling, *Mol. Phys.*, **100** (2002), 3285–3306.

[30] D. J. Wales, Some further applications of discrete path sampling to cluster isomerization, *Mol. Phys.*, **102** (2004), 891–908.

[31] D. J. Wales, Energy landscapes: calculating pathways and rates, *International Review in Chemical Physics*, **25** (2006), 237–282.

[32] The database for the Lennard-Jones-38 cluster, `http://www-wales.ch.cam.ac.uk/examples/PATHSAMPLE/`.

[33] Wales group web site `http://www-wales.ch.cam.ac.uk`.

[34] D. J. Wales and J. P. K. Doye, Global Optimization by Basin-Hopping and the Lowest Energy Structures of Lennard-Jones Clusters containing up to 110 Atoms, *J. Phys. Chem. A*, **101** (1997), 5111–5116.

[35] D. J. Wales, M. A. Miller and T. R. Walsh, Archetypal energy landscapes, *Nature* , **394** (1998), 758–760.

[36] D. J. Wales, *Energy Landscapes: Applications to Clusters, Biomolecules and Glasses*, Cambridge University Press, 2003.

[37] D. J. Wales and P. Salamon, Observation time scale, free-energy landscapes, and molecular symmetry, *Proc. Natl. Acad. Sci. USA*, **111** (2014), 617–622.

[38] A. D. Wentzell, Ob asimptotike naibol'shego sobstvennogo znacheniya ellipticheskogo differentsial'nogo operatora s malym parametrom pri starshikh proizvodnykh, (Russian) *[On the asymptotics of the largest eigenvalue of the elliptic differential operator with a small parameter at the highest derivatives], Dokl. Akad. Nauk SSSR*, **202** (1972), 19–21.

[39] A. D. Wentzell, On the asymptotics of eigenvalues of matrices with elements of order $\exp\{-V_{ij}/2(\epsilon^2)\}$, *Soviet Math. Dokl.*, **13** (1972), 65–68.

Received February 2014; revised June 2014.

E-mail address: cameron@math.umd.edu